# DETECTION OF HEMORRHAGE AND EXUDATES IN RETINAL FUNDUS IMAGE OF DIABETIC PATIENTS

SITI SARAH BINTI AHMAD MANSOR

UNIVERSITI MALAYSIA PAHANG

# DETECTION OF HEMORRHAGE AND EXUDATES IN RETINAL FUNDUS IMAGE OF DIABETIC PATIENTS

SITI SARAH BINTI AHMAD MANSOR

This thesis is submitted as partial fulfilment of the requirements for the award of the Bachelor of Electrical Engineering (Hons.) (Electronics)

Faculty of Electrical & Electronics Engineering
Universiti Malaysia Pahang

DECEMBER 2016

# UNIVERSITI MALAYSIA PAHANG

**DECLARATION OF THESIS AND COPYRIGHT**

| | | |
|---|---|---|
| Student's Full Name | : | SITI SARAH BINTI AHMAD MANSOR |
| Identification Card No | : | 930402-10-6774 |
| Title | : | DETECTION OF HEMORRHAGE AND EXUDATES IN RETINAL FUNDUS IMAGE OF DIABETIC PATIENTS |
| Academic Session | : | SEMESTER 1 SESSION 2016/2017 |

I declare that this thesis is classified as:

| | | |
|---|---|---|
| ☐ | **CONFIDENTIAL** | (Contains confidential information under the Official Secret Act 1972) |
| ☐ | **RESTRICTED** | (Contains restricted information as specified by the organization where research was done)* |
| ☑ | **OPEN ACCESS** | I agree that my thesis to be published as online open access (Full text) |

I acknowledge that Universiti Malaysia Pahang reserve the right as follows:

1. The Thesis is the Property of University Malaysia Pahang.
2. The Library of University Malaysia Pahang has the right to make copies for the purpose of research only.
3. The Library has the right to make copies of the thesis for academic exchange.

Certified by:

sarah mansor

(Student's Signature)

930402-10-6774

Date: 4TH JANUARY 2017

(Supervisor's Signature)

DR. ROSDIYANA BINTI SAMAD

Date: 4TH JANUARY 2017

## SUPERVISOR'S DECLARATION

I hereby declare that I have checked this thesis and in my opinion, this thesis is adequate in terms of scope and quality for the award of the degree of the Bachelor Degree of Electrical Engineering (Hons.) (Electronics).

| | | |
|---|---|---|
| Signature | : |  |
| Name of Supervisor | : | DR. ROSDIYANA BINTI SAMAD |
| Position | : | SUPERVISOR |
| Date | : | 4TH JANUARY 2017 |

## STUDENT'S DECLARATION

I hereby declare that the work in this thesis is my own except for quotations and summaries which have been duly acknowledged. The thesis has not been accepted for any degree and is not concurrently submitted for award of other degree.

| | | |
|---|---|---|
| Signature | : | *sarah mansor* |
| Name | : | SITI SARAH BINTI AHMAD MANSOR |
| ID Number | : | ED12049 |
| Date | : | 4TH JANUARY 2017 |

**All the effort that has been put in this work is dedicated to my beloved mother,**
**Nor ‘Aini binti Ramly and my late grandfather, Ramly bin Rathwan.**
**Mama, I love you. Atok, I miss you.**

## ACKNOWLEDGMENTS

Alhamdulillah, all praises to Allah, the most merciful and the most benevolent. Thank you Allah for granting me the strength and giving me ideas in completing the journey of Projek Sarjana Muda (PSM) and to finish writing the thesis.

I would like to express my greatest gratitude to my beloved mother for her prayers and unlimited support. Without her, it would be impossible for me to achieve anything in life. Her love is all that makes me keep moving on.

This work also would not have been completed without support from the supervisor of this project, Dr. Rosdiyana binti Samad for her endless encouragement and concern in my study to finish the project for PSM 1 and PSM 2.

Lastly, I want to harness this little chance that I had to acknowledge all the people out there who never gave up and keep moving forward despite of all the challenges that could have bring them down. Mental breakdown is common in life and everyone had to face it, but how we managed our emotion defines who we are. So, whenever problem hits us, let's keep our chin up because we are our own hero.

## ABSTRACT

Diabetes is a disease that interferes with the body's ability to use and store sugar, which can cause many health problems. Over time, diabetes affects the circulatory system including the retina. As diabetes progress, the vision of a patient may start to deteriorate and then leading to Diabetic Retinopathy (DR) which further will cause blindness. So, early detection of the disease is important to avoid blindness. There are several ways to diagnose DR and slit – lamp examination is one of the traditional method used by the ophthalmologist. This method requires the clinician to see directly into patient's eye through an ophthalmoscope or the slit lamp machine to determine whether or not the eyes contain any abnormal features that indicate DR. However, this is not the most effective method yet. Any human can get tired and drowsy including doctors. This natural flaws of human being can affect the diagnosis and then causing false result analysis. Besides, every individuals doesn't hold same opinion and judgment. Therefore, this project is proposed to assist the clinicians in identifying DR. There are two main abnormal features that are formed in the retina of a diabetic retinopathy's patient. They are hemorrhage and exudates. Hemorrhage are formed as a result due to leakage of retinal blood vessel which has similar red colour to the vessel. Whereas exudates are yellow-white deposits structure on the retina that is formed due to leakage of blood from abnormal vessels. This thesis mainly focuses on developing a Fundus Image Analysis (FIA) system that extracts the anatomical and both the abnormal features of the retina in order to diagnose the disease. This research is carried out in three phases. In the first phase, an automated system is developed to distinguish the anatomical features of the retina from the abnormal features. This phase is called the Masking Phase. This phase involved combinations of several image processing techniques including Specify Polygonal Region of Interest (ROIPOLY), Contrast-limited adaptive histogram equalization (CLAHE), Morphological Opening and Structuring, Median Filtering and Thresholding. The second phase is the Haemorrhage Extraction phase. In this phase, Saturation Adjust Method, Morphological operations and Regional Minima technique is proposed. The third and the last phase is the Exudates Extraction phase. In this phase, Edge Detection, Gradient Magnitude and Region Of Interest techniques are combined to form a complete working algorithm. The experimented images in this project are the retinal fundus images that was taken from a public database (diaretdb1 - Standard Diabetic Retinopathy Database). It is a public database for benchmarking diabetic retinopathy detection from digital images. By using this database and the defined testing protocol, the results between different methods can be compared. At the end of this project, the result shows that the method applied is able to detect exudates features and capable of detecting and distinguishing hemorrhage from blood vessels. Final result shows the accuracy of 48.3% for detecting images with haemorrhages and 68.5% for images with exudates.

# ABSTRAK

Diabetis merupakan sejenis penyakit yang boleh menganggu keupayaan tubuh manusia untuk menggunakan dan menyimpan gula dalam darah. Penyakit diabetis juga boleh menganggu sistem saliran darah termasuk saliran darah pada retina mata. Untuk suatu jangka waktu, diabetis boleh mengakibatkan sistem penglihatan pesakit mula terganggu dan hal ini akan membawa kepada penyakit *diabetic retinopathy* yang juga boleh menyebabkan hilangnya penglihatan secara kekal jika tidak dirawat. Mengenalpasti penyakit ini pada peringkat awal adalah penting untuk mengelakkan pesakit daripada menjadi buta. Terdapat beberapa kaedah untuk mendiagnos penyakit *diabetic retinopathy* ini dan salah satu daripadanya adalah pemeriksaan *slit – lamp*. Kaedah ini memerlukan doktor terlatih untuk melihat ke dalam mata pesakit secara terus dengan menggunakan sejenis mesin iaitu *ophthalmoscope* untuk mengenalpasti ciri – ciri tidak normal pada retina mata pesakit tersebut. Walaupun kaedah ini terbukti berkesan, namun ia masih tidak mencukupi. Manusia mengalami rasa mengantuk dan kepenatan termasuk para doktor. Kelemahan alami pada manusia ini secara tidak sedar boleh memberi kesan terhadap pemerhatian diagnosa dan akhirnya membawa kepada konklusi yang salah. Tambahan pula, tidak semua individu mempunyai pendapat dan penilaian yang sama. Oleh itu, projek ini diutarakan untuk membantu para doktor dalam mengenalpasti penyakit ini. Terdapat dua ciri – ciri tidak normal utama yang terbentuk pada retina mata pesakit *diabetic retinopathy*. Ciri – ciri tersebut adalah *hemorrhage* dan *exudates*. *Hemorrhage* terbentuk daripada saluran darah mata normal yang pecah. Oleh itu, *hemorrhage* mempunyai ciri warna yang sama dengan sesalur darah, iaitu warna merah. Manakala *exudates* merupakan struktur kekuningan yang terbentuk daripada saluran darah mata tidak normal yang pecah. Daripada maklumat asaas ini, teknik pemprosesan imej dilakukan untuk mengenalpasti *hemorrhage* dan *exudates*. Tesis ini memfokuskan pembangunan sistem Analisis Imej Fundus yang mengenalpasti ciri – ciri anatomi dan ciri – ciri tidak normal pada retina mata supaya penyakit *diabetic retinopathy* dapat dikesan. Kajian ini dijalankan dalam tiga fasa. Dalam fasa pertama, sistem automatik dibangunkan untuk membezakan ciri – ciri anatomi retina daripada ciri-ciri yang tidak normal. Fasa ini dipanggil *Masking Phase*. Fasa ini melibatkan gabungan beberapa teknik pemprosesan imej termasuk *Specify Polygonal Region of Interest (ROIPOLY), Contrast-limited adaptive histogram equalization (CLAHE), Morphological Opening* dan *Morphological Structuring, Median Filtering dan Thresholding*. Fasa kedua adalah pengekstrakan *hemorrhage.* Algoritma yang dibangunkan dalam fasa ini melibatkan *Saturation Adjust, Morphological Operations* dan *Regional Minima*. Fasa ketiga dan terakhir bagi sistem automatik ini adalah pengekstrakan *exudates*. Dalam fasa ini, *Edge Detection, Gradient Magnitude* dan *Region of Interest* digabungkan untuk membentuk satu algoritma lengkap. Imej – imej yang digunapakai dalam projek ini adalah imej fundus retina yang diambil daripada pangkalan data awam (diaretdb1 - Standard Diabetic Retinopathy Database). Ia adalah pangkalan data awam yang bertindak sebagai penanda aras untuk mengesan penyakit *diabetic retinopathy* daripada imej digital. Dengan menggunakan pangkalan data ini dan protokol ujian yang telah ditentukan, keputusan antara kaedah yang berbeza boleh dibandingkan. Pada akhir projek ini, analisa menunjukkan bahawa kaedah yang digunapakai mampu mengesan *exudates* dan mampu mengesan dan membezakan *hemorrhage* dari pembuluh darah. Keputusan akhir menunjukkan ketepatan 48.3% untuk mengesan imej dengan *hemorrhage* dan 68.5% untuk imej dengan *exudates*.

# TABLE OF CONTENTS

# LIST OF TABLES

# LIST OF FIGURES

## LIST OF ABBREVIATIONS

| | |
|---|---|
| FIA | Fundus Image Analysis |
| CAD | Computer Aided Diagnosis |
| DR | Diabetic Retinopathy |
| ROIPOLY | Specify Polygonal Region Of Interest |
| ROI | Region of Interest |
| GUI | Graphical User Interface |
| GUIDE | Grapical User Interface Development Envirenment |

# CHAPTER 1

# INTRODUCTION

## 1.1 INTRODUCTION

Medical imaging is a methods of creating visual representation of the interior part of human body for medical analysis. Medical imaging creates database of normal anatomy and physiology to enables abnormalities identification so that it can be used for diagnosing and treating diseases. Computer Aided Diagnosis (CAD) is being developed to translate a medical image into an outcome that are able to help physicians understand more about a disease with a more accurate findings. Besides, this application can run in shorter time and less human effort can be used. The most established CAD applications in medical fields are the automated systems in mammography, chest computed tomography and radiography.

This thesis describes the algorithm that can aid in the detection of diabetic retinopathy. Diabetic Retinopathy (DR) is an eye disease that happens due to complication of diabetes. DR can causes vision loss if left untreated at the early stage. To properly and correctly detecting the disease, an automated detection system is needed. Therefore, the aid of a computer is needed to interpret and analyse the digital images of the retina.

The Fundus Image Analysis (FIA) system described in this thesis is developed to assist the ophthalmologists by providing reference to their diagnosis. To study diabetic retinopathy, doctors use Colour fundus image to begin with. From here, extraction of anatomical features and abnormal features can be done according to desired outcome.

## 1.2 DIABETIC RETINOPATHY

Diabetic Retinopathy (DR) is a complication of diabetes on retina that occurs because of the microangiopathy which in turn affects the retinal precapillary arterioles, capillaries and venules. It is mainly caused by leakage of the microvascular. Progressive damage of the microvascular can cause permanent vision loss can happen.

Microaneurysms are the first clinically noticeable signs of diabetic retinopathy. High sugar levels in the blood causes the walls of small blood vessels to swell thus creating this microaneurysms. As the disease progresses, microaneurysms will be ruptured. This will then cause the formation of hemorrhage. Retinal hemorrhage look either as small red dots or spots identical to microaneurysms. Exudates formed through vessels leakage of lipids and proteins. They are seen on the retina as typical bright, reflective white or yellowish coloured lesions.

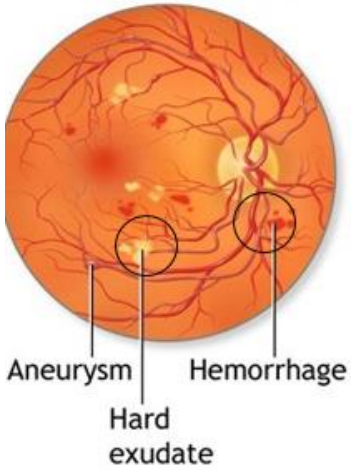


**Figure 1.1:** Illustration of retinal microaneurysm, hemorrhage and exudates.

In Malaysia, 3.3 million cases of diabetes is recorded in the year of 2015. With the rising prevalence of diabetes mellitus worldwide, diabetic retinopathy is now a leaking cause of blindness among working age individuals. Early detection and treatment is of vital importance as it may prevent vision loss and blindness (Vashist, Singh et al. 2011).


**Figure 1.2:** Illustration of normal vision versus vision with diabetic retinopathy

## 1.3 CONVENTIONAL SCREENING METHOD FOR DIABETIC RETINOPATHY

Early detection and treatment of diabetic retinopathy can prevent visual impairment and most of the patients can be saved from vision loss. Screening is an effective way for early detection of diabetic retinopathy. Studies have revealed that people who suffer from diabetes benefit from regularly attending a screening session (Bresnick, Mukamel et al. 2000). In this screening session retinas of both eyes are examined by an ophthalmologist. If diabetic retinopathy is detected, patient can continue with follow up.

Traditionally the screening session requires the ophthalmologist to observed the retina either directly using an ophthalmoscope or indirectly through digital photographs taken from a fundus camera. Ophthalmoscope is an instrument containing a light source and lenses. Whereas s digital fundus camera is a low power microscope with a camera attached and designed to take picture of the interior parts of the eye. For large scale screening, fundus images are more reliable than ophthalmoscope in detecting diabetic

retinopathy features (Wendt, Rönnholm et al. 2000). This is because, digital fundus photography allows instant examination of the retina plus the image storage can be accessed at any time.

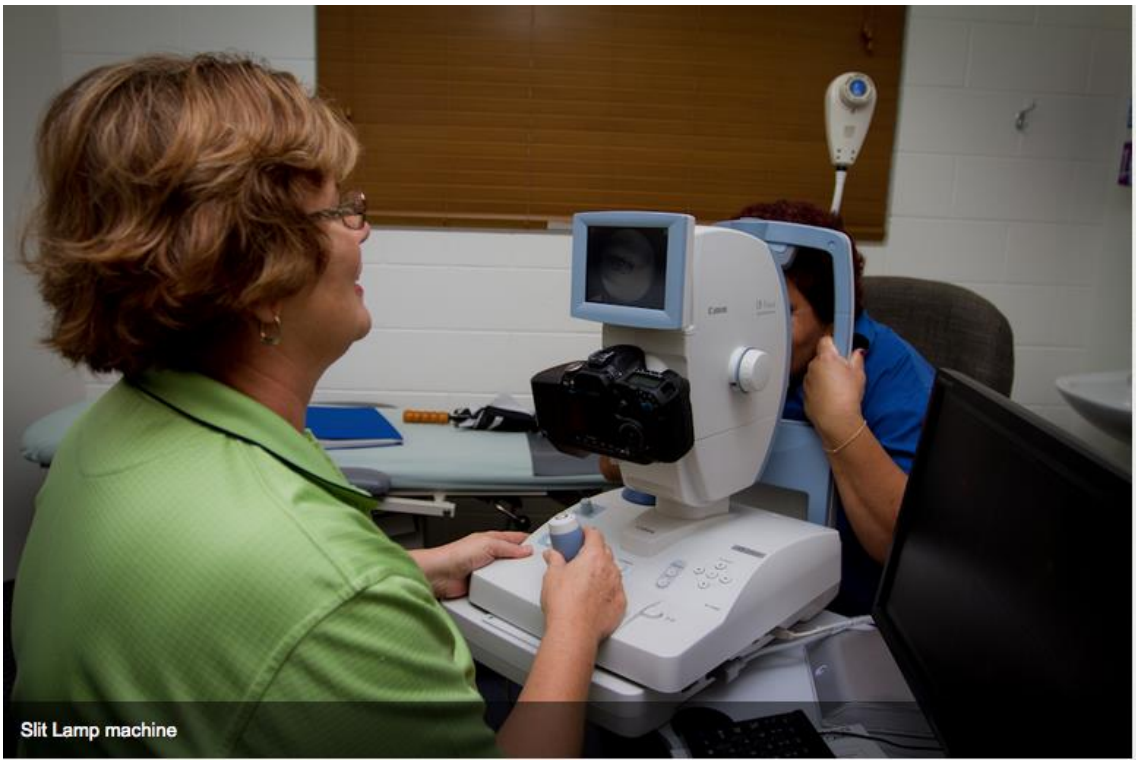


**Figure 1.3:** Slit – lamp ophthalmoscopy

## 1.4 PROBLEM STATEMENT

Screening methods that needed medical examiner to examine directly using Ophthalmoscope are vulnerable and the diagnosed result might be incorrect due to false judgment depending on different examiners.

According to a review paper in this area of study in 2012, it mentioned that it is very difficult to detect exudates clearly, because they are such tiny spots on the retina. Also, the detection of hemorrhages is very challenging. The texture of hemorrhages and macula is almost the same (Faust, Acharya U. et al. 2012). Therefore, a robust algorithms

which able to detect these features with 100 percent accuracy is still needed to be developed.

## 1.5 OBJECTIVES OF STUDY

The objectives of this project is to develop an algorithm for hemorrhage and exudates detection using image processing techniques so that it can be used to assist Ophthalmologist in determining Diabetic Retinopathy disease. A MATLAB based Graphic User Interface (GUI) will act as an interactive tools for the clinicians to use.

## 1.6 SCOPES OF STUDY

In this project, the study focuses on detection of haemorrhage and exudates feature of diabetic retinopathy disease even though there are other features that are present as a symptom of this disease. This is because, these two features are the most visible feature of diabetic retinopathy at the early stage.

The sample image that is used in this study is the colour fundus image downloaded from a Standard Diabetic Retinopathy Database (DIARETDB1) (Tomi Kauppi, Valentina Kalesnykiene et al. 2007). This public database provided 89 sample fundus images with marked ground truth for result comparison.

# CHAPTER 2

# LITERATURE REVIEW

## 2.1 INTRODUCTION

Automated screening system such as Diabetic Retinopathy Screening System has been increasingly established since years ago. This kind of system delivers huge contribution to the medical world especially in doing research findings and providing treatments to a number of large scale patients. Image processing now one of the most useful and important tool for diabetic retinopathy screening. However, fundus image analysis using image processing techniques is a complicated task, because of the variability of the fundus images in terms of colour or grey levels, the morphology of the anatomical structures of the retina and the existence of certain features in different patients that may lead to a wrong interpretation.

This chapter discussed the contribution of Computer Aided Diagnosis (CAD) technology in medical field. After that, simple overview of the anatomy of the eye is made followed by a review of hemorrhage and exudates detection approach.

## 2.2 TECHNOLOGY IN COMPUTER AIDED DIAGNOSIS

Computer Aided Diagnosis (CAD) are the systems that assist clinicians in interpreting digital medical images. This technology combines the elements of artificial intelligence, machine vision and image processing to produce one complete automated system. Recently, CAD is beginning to be applied widely in the detection and differential diagnosis of many different types of abnormalities in medical images obtained in various examinations by use of different imaging modalities (Doi 2007). The contributions of CAD, which is in the early stages of implementation, to complex image interpretation in mammography and to all fields of medicine is likely to be substantial (Burhenne, Wood et al. 2000).

Large scale and systematic research and development of various CAD schemes were begun in the early 1980s at the Kurt Rossmann Laboratories for Radiologic Image Research in the Department of Radiology at the University of Chicago. Based on Radiological Society of North America meeting in the year of 2000 to 2005, majority of the presentations were concerned with three organs which are the chest, breast and colon but other organs such as brain, live, skeletal and vascular system were also subjected to CAD research (Doi 2007).

In recent years, numerous studies had been done to evaluate the performance of comprehensive CAD system for diabetic retinopathy (DR) screening compared to the human expert performance. From these studies, the performance of the system is said to be comparable to that of human experts. Besides, the system offers retinopathy screening programs a fast solution to reduce the burden of screening diabetes population while maintaining a high sensitivity (Sánchez, Niemeijer et al. 2011). In another research, it was said that their developed automated screening system for DR was able to differentiate between a normal fundus and a fundus with DR. They also mention that the program reduces the clinician's workload and the retinal image can be interpreted immediately (Singalavanija, Supokavej et al. 2006).

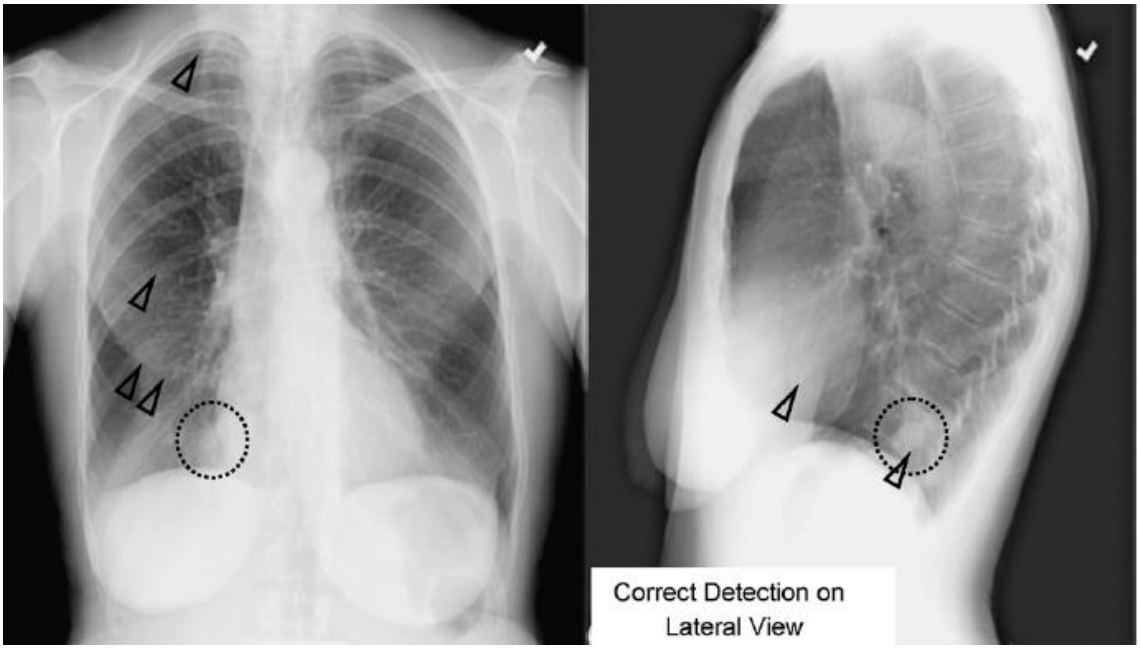


**Figure 2.1:** Illustration of a relatively large, but very subtle lung nodule (dotted circles) located in the right mediastinum region which was correctly marked by CAD

Image acquisition is one of the most important stage to begin with a CAD system development. As for DR, there are a lot of imaging techniques that can be useful depending on the manifestation of disease. Some of the important techniques are color fundus photography, fluorescein angiography (FA), B-scan ultrasonography and optical coherence tomography (OCT). According to (Salz and Witkin 2015), fundus photography can be used to document retinal disease over time, and may be increasingly helpful in screening of diabetic patients for retinopathy. They also added that Pros of this form of color photography include that it is easy to use and highly available, and can be utilized to assist in documentation. Certain morphologic features such as hard exudates are easy to identify on color photographs.

## 2.3 ANATOMY OF THE EYE

The eye is one of the most complex organs of the human body. In the human eye, three layers can be distinguished . The schematic illustration of the structure of the eye is shown in figure 2.2. The outer region consists of the cornea and the sclera. The cornea refracts and transmits the light to the lens and the retina and protects the eye against infection and structural damage to the deeper parts. The sclera forms a connective tissue coat that protects the eye from internal and external forces and maintains its shape. The cornea and the sclera are connected at the limbus. The visible part of the sclera is covered by a transparent mucous membrane, the conjunctiva. The middle layer of the eye is composed of the iris, the ciliary body and the choroid. The iris controls the size of the pupil, and thus the amount of light reaching the retina; the ciliary body controls the power and shape of the lens and is the site of aqueous production; and the choroid is a vascular layer that provides oxygen and nutrients to the outer retinal layers. The inner layer of the eye is the retina, a complex, layered structure of neurons that capture and process light. The three transparent structures surrounded by the ocular layers are called the aqueous, the vitreous and the lens (Willoughby, Ponzin et al. 2010).

Macula located at the centre of the retina, opposite to the optic disk. It is responsible to have fine central vision and colour vision. The centre of macula is called fovea. This is the most sensitive region of the retina. Macula is about 4 to 5mm thick, which enable human to see details and doing meaningful tasks, like reading. Features of macula and fovea can be seen in figure 2.3. In the figure, optic disk is the bright yellowish disk located at the front of the retina. Here, blood vessels and optic nerve fibres emerge. Optic disk measures 1.5 to 2 mm in diameter.

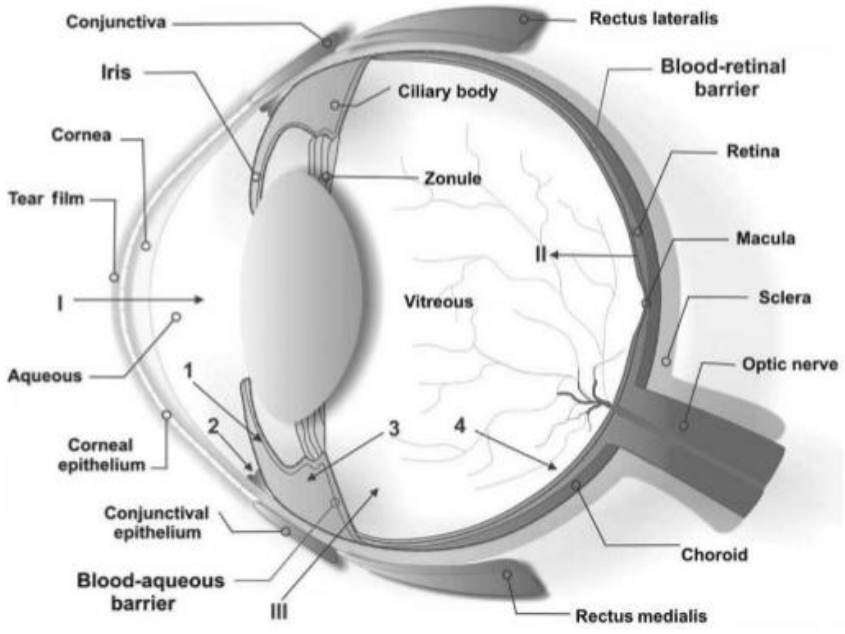


**Figure 2.2:** Schematic illustration of the structure of the eye and the ocular barriers (Willoughby, Ponzin et al. 2010).

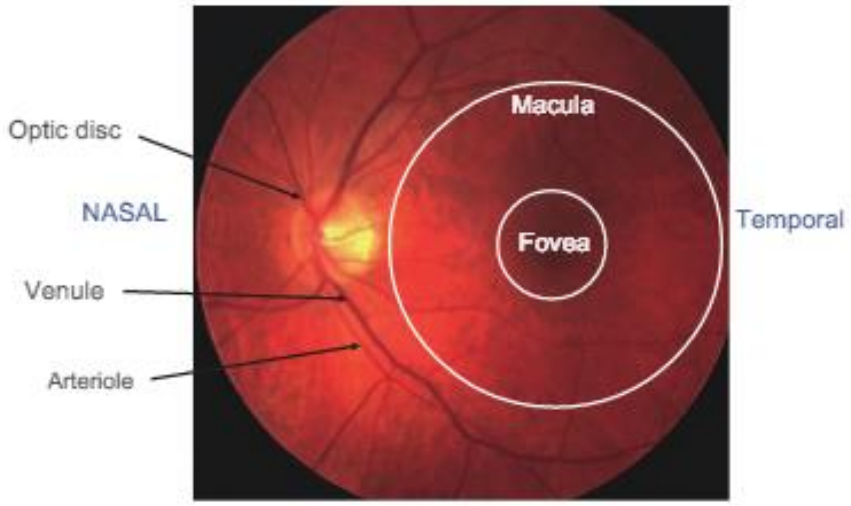


**Figure 2.3:** The fundus of the eye showing the macula, the fovea and the optic disc (Willoughby, Ponzin et al. 2010).

The retinal blood vessels are originated from the central retinal artery and vein that lie in the optic nerve head. These blood vessels nourish the internal parts of retina and radiate out from the optic disk.

In detecting DR, retina is the most important part. The specific vascular changes caused by diabetic retinopathy can often be detected visually by examining the retina (Willoughby, Ponzin et al. 2010). The retina is the tissue that lines the inner surface of the eye, surrounding the vitreous cavity. The retina is the tissue that lines the inner surface of the eye, surrounding the vitreous cavity (Willoughby, Ponzin et al. 2010).

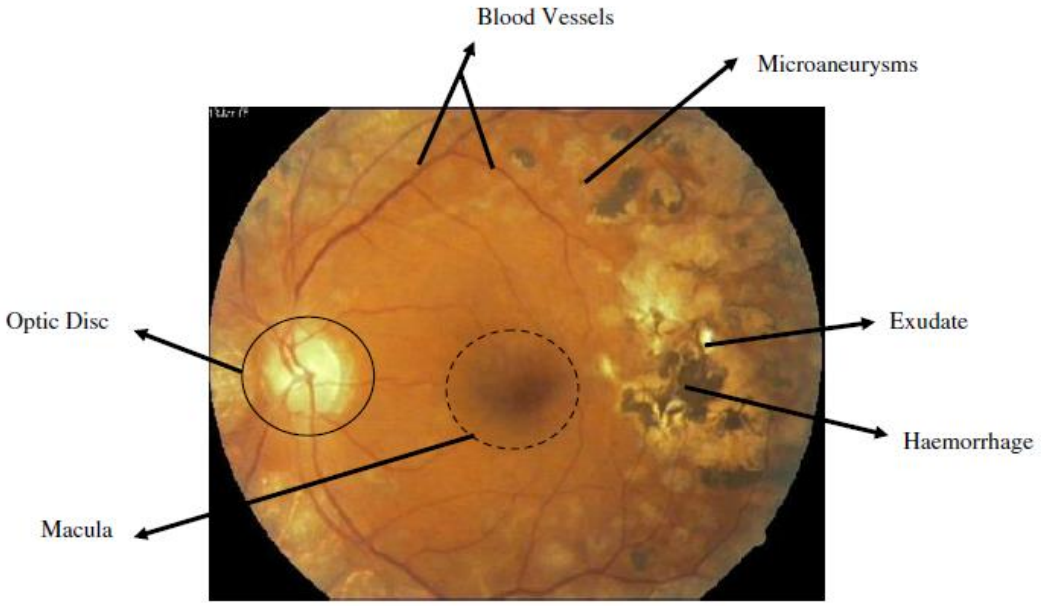


**Figure 2.4:** Different features in a DR image (Faust, Acharya U. et al. 2012)

Microaneurysms are small saccular pouches caused by local distension of capillary walls and appear as small red dots. This may form lead to big blood clots called hemorrhages (Ravishankar, Jain et al. 2009).

Retinal hemorrhages are caused by retinal ischemia and primarily caused by abnormally fragile blood vessels in hypertension, malaria and primarily, preproliferative

and proliferative DR. Large hemorrhages are asymptomatic except when they are located in the center of the macula. Compared with anatomical structures, such as optic disc, fovea and blood vessels, the shape and appearance of hemorrhages show substantial variability (Tang, Niemeijer et al. 2013) .

Hard exudates in the fundus image are yellowish intraretinal deposits, which are usually located in the posterior pole of the fundus. This features is made up of serum lipoproteins, thought to leak from the abnormally permeable blood vessels, especially across the walls of leaking microaneurysms. They are often seen in either individual streaks or clusters or in large circinate rings surrounding clusters of microaneurysms (Walter, Klein et al. 2002).

## 2.4 REVIEW OF HEMORRHAGE DETECTION APPROACH

As hemorrhages consist of blood, they share appearance features with intravascular blood. That makes it difficult to differentiate these from retinal vessels using low level pixel features. On the contrary, by upgrading samples for classification from pixel level to splat level, information is encoded at the splat level, with less disturbance from pixel level noise. Thus, L. Tang and M. Niemeijer in their research presented a splat-based feature classification algorithm with application of hemorrhage detection in fundus photographs (Tang, Niemeijer et al. 2013). Splat-based feature classification is able to model shapes of various lesions efficiently regardless of their variability in appearance, texture or size. However, their approach produce many false positives outcome because many of the hemorrhages are connected with the retinal vessels.

Microaneurysm and hemorrhage can be detected applying the double-ring filter on the green channel of the color images, followed by the elimination of lesions in the blood vessels (Mizutani, Muramatsu et al. 2009). Using this method, false positives detected in the images can be grouped into two major categories, capillary blood vessel regions that were not identified as the regions corresponding to the blood vessels and noise regions

Hipwell, J. H. and Strachan, F. proposed a method for the detection of microaneurysms in red-free images (Hipwell, Strachan et al. 2000). The images were initially processed by shade correction of the image, followed by removal of vessels and other distractors by the top-hat transformation. A Gaussian matched filter was applied to retain candidate microaneurysms for subsequent classification. The images were graded for presence/absence of microaneurysms and/or hemorrhages against the reference standard of an experienced clinical research fellow.

Morphological processing algorithms are the most commonly used algorithms for hemorrhage detection. In 2006, Zhang and Xin Fan presented a spot lesion detection algorithm using multi scale morphological processing (Zhang and Fan 2006). The algorithm was tested on 30 retinal images and it achieved the sensitivity and predictive value of 84.10% and 89.20% respectively.

## 2.5 REVIEW OF EXUDATES DETECTION APPROACH

Exudates are accumulations of lipid and protein in the retina. Typically they are bright, reflective, white or cream colored lesions seen on the retina. They indicate increased vessel permeability and an associated risk of retinal edema. Although, not sight threatening in themselves, they are a marker of fluid accumulation in the retina (Faust, Acharya U. et al. 2012).

Sopharak and Akara Uyyanonvara in their research proposes an exudate detection techniques based on mathematical morphology on retinal images of non-dilated pupils that are low quality images (Sopharak, Uyyanonvara et al. 2008). This technique is very fast and requires lower computing power. There are also some incorrect exudate detections which are caused by the artefacts that are similar to exudates, artefacts from the noise in the image acquisition process, the exudates that are proximate to blood vessels or because the exudates appear very faint. However, the performance of the algorithm can be improved if these set of low-contrast exudates can be detected.

Due to significant gray level change in the whole image, it is very difficult to find a global threshold which can distinguish the exudates from the background. Therefore a ‘dynamic thresholding’ algorithm which calculates every pixel’s threshold according to its local histogram, is proposed and the results are promising (Zheng, Opas et al. 1997).

Exudates appear as bright lesions in retinopathy images and have sharp edges and high contrast with the background. Most of the standard edge detectors like Sobel and Canny add a lot of noise and miss out key edges when used for extracting exudate edges and hence are not suitable for this application (Ravishankar, Jain et al. 2009). In their research work, morphological operations for detecting boundary of exudates.

In a research by Biran and A Bidari, exudates are extracted by using a combination of Contrast-limited adaptive histogram equalization (CLAHE) image and two dimensional Gabor filter image followed by a thresholding techniques (Biran, Bidari et al. 2016). This proposed technique successfully detect the hard exudates and soft exudates.

## 2.6 SUMMARY

After reviewing variable techniques that has been proposed and based on their performances, this project is proceed by performing the algorithm that is best suited this case. For hemorrhage detection, morphological operations were applied and for exudates detection, predefined 2-D Prewitt filter is proposed.

# CHAPTER 3

# METHODOLOGY

## 3.1 INTRODUCTION

This chapter discusses the algorithm applied in this research work. The developed system can be divided into three phases. The first phase is the masking phase, the second phase is hemorrhage extraction phase and the third phase is exudates extraction phase. The algorithm is developed and justified by taking into account the important information and details from the previous studies in order to make the project success. The project is done part by part starting with writing the MATLAB coding for masking phase followed by hemorrhage and exudates extraction phase.

The process of automatic diabetic retinopathy detection involves detection and segmentation of the abnormal features from the input images. The general block diagram for the automatic diabetic retinopathy detection is shown below.


**Figure 3.1:** General Block Diagram for Diabetic Retinopathy Detection System

## 3.2 DATA COLLECTION

In this project, a number of 89 sample fundus images is tested. The images were downloaded from a Standard Diabetic Retinopathy Database (DIARETDB1). This public database provides benchmarking for diabetic retinopathy detection from digital images. By using this database and the defined testing protocol, the results between different methods can be compared.

The database consists of 89 colour fundus images of which 84 contain at least mild non-proliferative signs of microaneurysms of the diabetic retinopathy, and 5 are considered as normal. Images were captured using the same 50 degree field-of-view digital fundus camera with varying imaging settings. The data correspond to a good practical situation, where the images are comparable, and can be used to evaluate the general performance of diagnostic methods.

Ground truth provided by this public database are marked by 4 medical experts were collected by using a software tool provided for image annotation. The experts were asked to mark the areas related to the microaneurysms, hemorrhages, and hard and soft exudates. The experts were further instructed to report their confidence and especially annotate the single most representative point for each finding. The ground truth confidence levels, (<50%,~>50%,~100%) represented the certainty of the decision that a marked finding is correct. Example of exudates and hemorrhage ground truth for a sample fundus image is shown in figure 3.2 below.

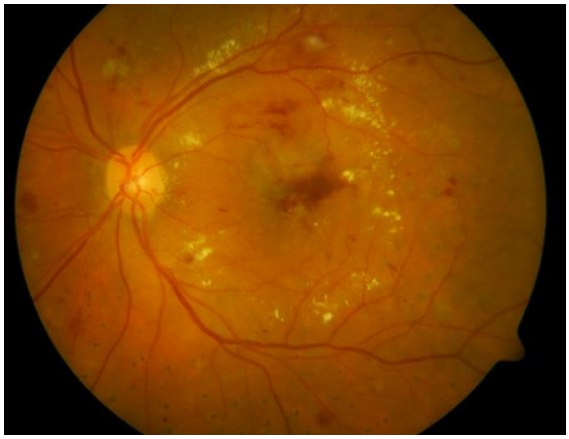

(a)

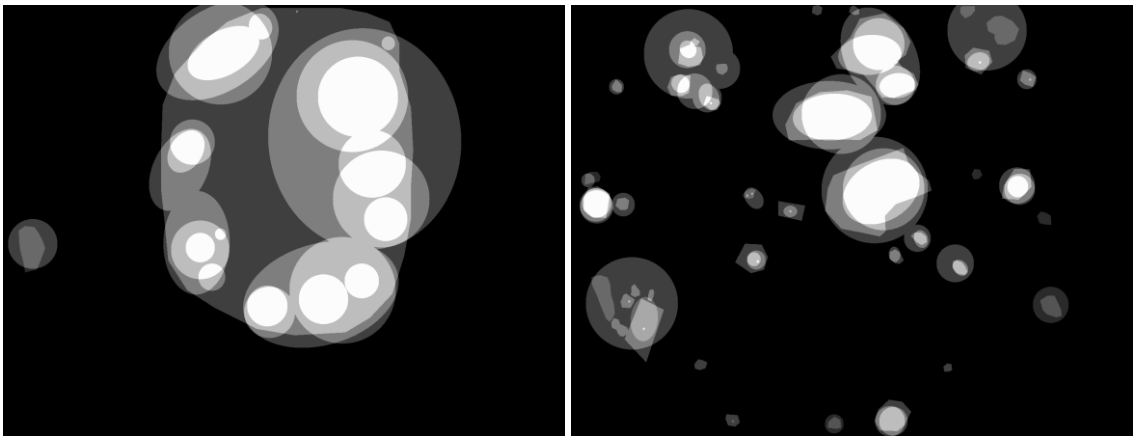

(b) (c)

**Figure 3.2:** Examples of ground truth provided from DIARETDB1 (a) original fundus image (b) exudates ground truth (c) hemorrhage ground truth

Figure 3.2 below shows the example of fundus images from DIARETDB1 comprises from normal image, image with haemorrhage and image with exudates.

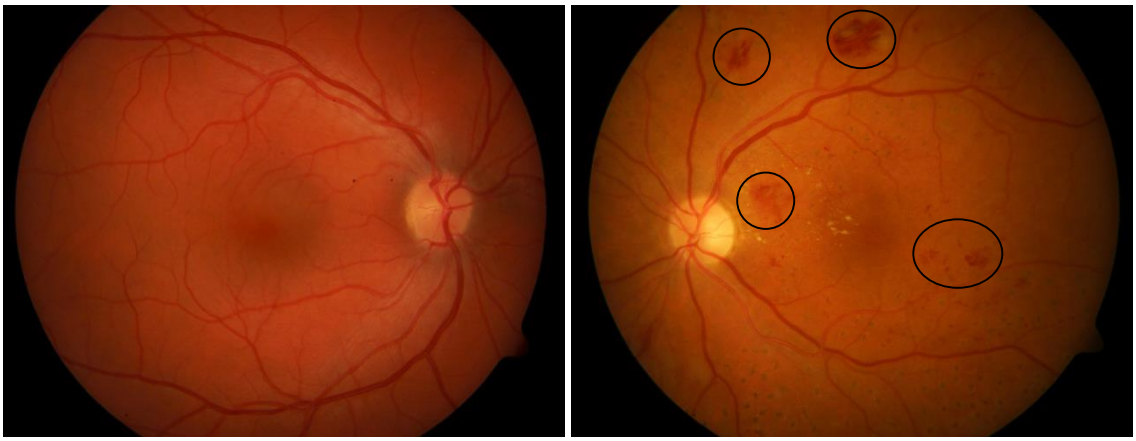

(a) (b)

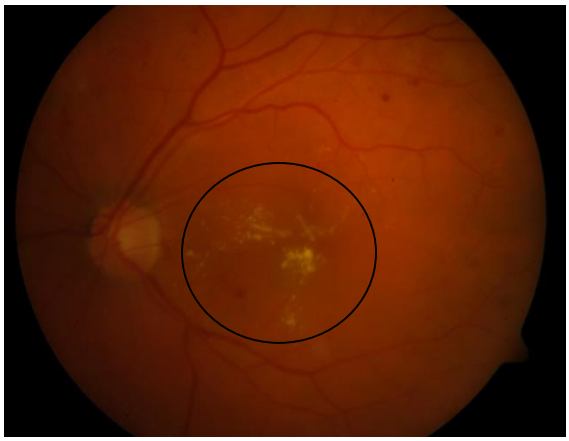

(c)

**Figure 3.3:** Sample images from DIARETDB1 (a) Normal Fundus Image (b) Image with Hemorrhage (c) Image with Exudates

## 3.3 HEMORRHAGE DETECTION ALGORITHM

In this section, the algorithm used for this project is discussed. The algorithm for detecting hemorrhage started with the masking phase and then proceed with image enhancement, feature extraction and decision making for deciding the feature detected.

### 3.3.1 Optic Disk, Retinal Background and Blood Vessel Masking

Colour is the most reliable parameter that can be used to perform image processing for this system. Both hemorrhage and exudates has fixed colour scheme to represent their trait. Hemorrhage is red in colour while exudates has yellowish colour (Mistry, Vikhe et al.). Based on this characteristic, it is easier to differentiate these features from one another by colour detection. Size and shape are highly vulnerable parameters as hemorrhage and exudates formed an irregular blob spots on the retina and these characteristics are not fix for every cases. Therefore, the only parameters that is considered in this project is colour.

However, it appear to be that the optic disk has same yellowish colour as exudates and the blood vessels has same red colour as hemorrhage. Segmenting the abnormal features could be confused by the colour of these anatomical features in the eye when colour image processing is done. To solve this problem, the optic disk and blood vessels need to be removed.

The proposed method for optic disk and blood vessels removal is through masking phase. In the masking phase, optic disk and blood vessels is detected and segmented. After that, both features are turned into binary image with selected features set to be black in colour. The idea of masking is to assign zero pixel value to the optic disk and the blood vessels so that when the mask is multiplied to an original image, optic disk and blood vessels are covered in black colour and it would be easier to differentiate their pixel value from hemorrhage and exudates features in grayscale image based on the pixel value.

**Optic Disk Masking**

Optic disk is a clearly visible feature of the optic nerve head within the retina. It is always brighter than the surrounding area besides having an elliptical shape. It is very easy to detect the optic disk with naked eye. Therefore in order to come out with the optic disk mask, specify polygonal region of interest (ROIPOLY) from MATLAB toolbox is used as part of the system.

Specify Polygonal Region of Interest (ROIPOLY) let user select any region of interest in polynomial shape by clicking around the object in number of points as desired. In this case, the region of interest is the optical disk. Basically the optic disk is in round shape. However, a rectangle is enough to cover the whole optical disk without removing any important detail from the surrounding. Therefore, the ROIPOLY is set to four points so it'll formed a rectangle shape. Now, the optical disk can be selected manually from the original image.

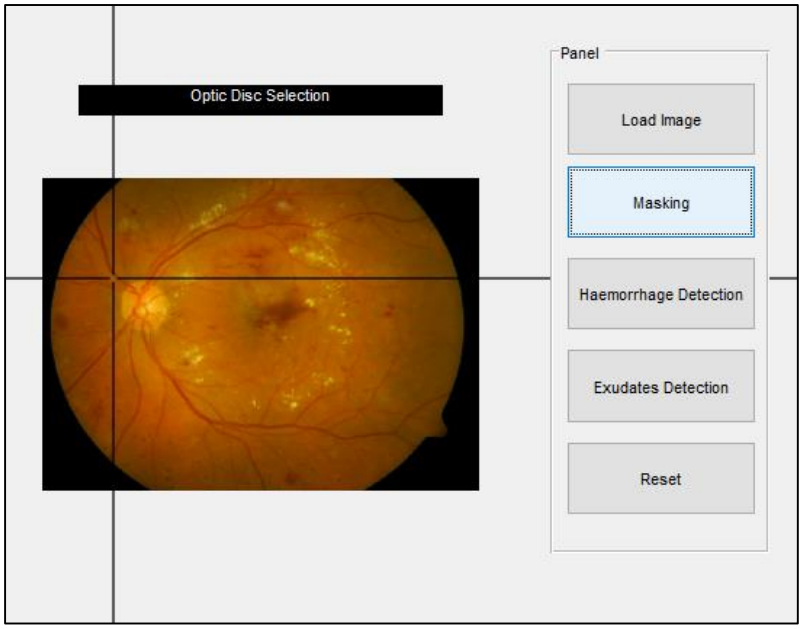


**Figure 3.3.1:** Optical Disk selection from designated GUI

The selected region will form a binary image as the new processed image. The image is then simply complemented to form a binary mask for the optical disk. Image (c) in figure 3.3.2 shows the example of masked optic disk on a grayscale image. This is done through a simple process of image multiplication technique using the complemented mask with its corresponding image in grayscale form.

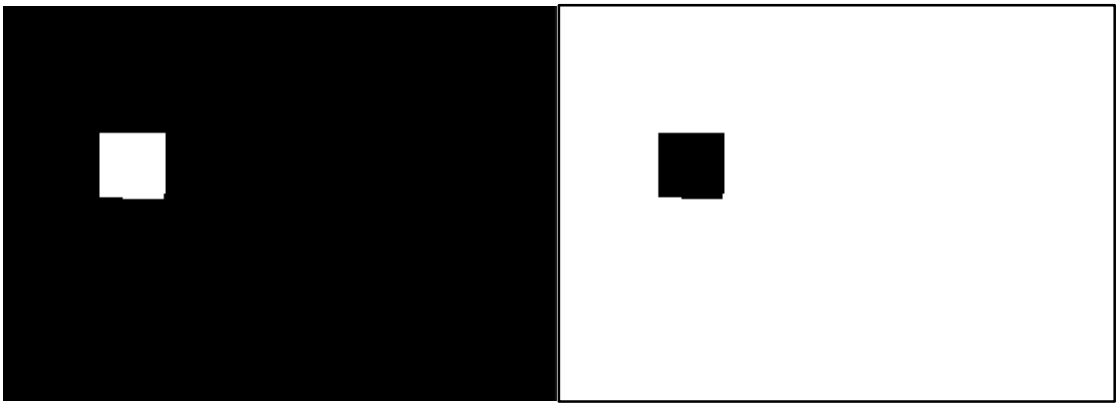

(a) (b)

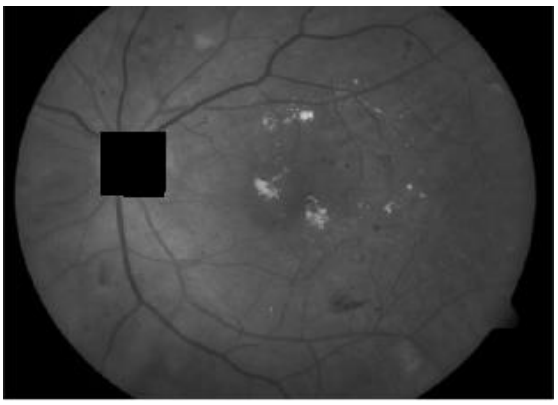

(c)

**Figure 3.3.2:** Output images of optical disk masking (a) selected region output image (b) complemented image (c) example of masked optic disk on a greyscale image

**Retinal Background Masking**

Background masking algorithm is developed to remove noise in colour retinal image. Noise occur in colour retinal image due to the pixel of distorted colour. This noise exist in the region of the image where it receives inadequate illumination. The centre of the image usually receives enough illumination hence making the edges of the retinal image become darker. This darker regions may have the potential to cause errors in abnormal features detection especially during the hemorrhage extraction. Therefore, it is very important to improve of the poor quality image at the beginning of work.

The aim of background masking is to have the edges of the retina to be covered with black colour which also mean to convert the edges to zero pixel value. To do that, first all Red, Green and Blue (RGB) channel of the fundus image is manually set to zero. The output image is already in binary in this part. After that, dilation is done to enlarge the boundaries of regions of foreground pixels typically white pixels. The dilation of A by B denoted by $A \oplus B$ is defined as the equation below.

$$A \oplus B = \{z|(\dot{B})z \cap A \neq \emptyset\}$$ (Kamarul HG, Nurul Wahidah A et al. 2016)

The image is then complemented to get the black pixel to be on the edge of the retina image. The background of object A is given by $A^c$ which also mean the complement of object A. This condition can be visualize through the equation below.

$$A^c = \{\propto | \propto \epsilon A\}$$ (Kamarul HG, Nurul Wahidah A et al. 2016)

The resultant image of retinal background masking is shown in figure 3.3.3 below.

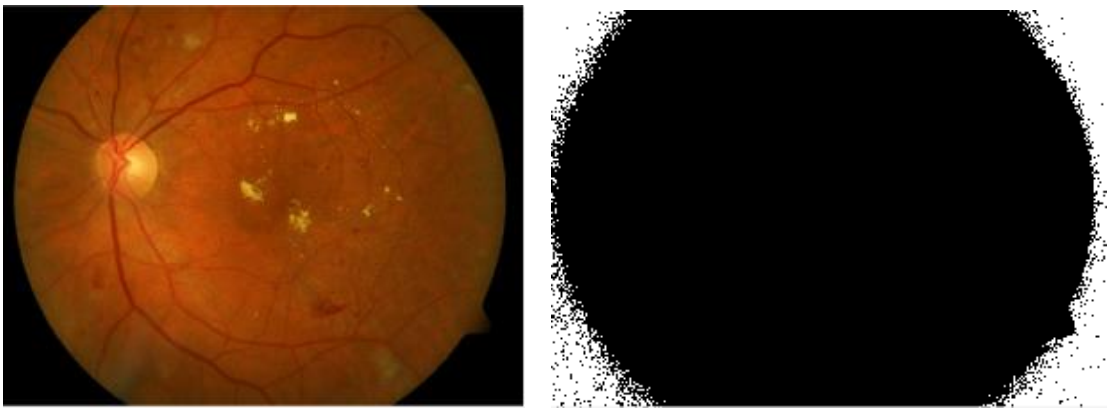

(a) (b)

(c)

**Figure 3.3.3:** Output images of retinal background masking (a) RGB fundus image (B) all RGB channel set to 0 pixel (c) complemented image

**Blood Vessels Masking**

The purpose of segmenting and masking blood vessels in the retina is to discriminate the blood vessels from hemorrhage as these features are having the same red colour. To start with the blood vessel masking, the green channel of the fundus image is extracted. As compared to grayscale image, red channel image and blue channel image,

green channel shows clearer detail of blood vessel with high contrast between the blood vessel network and the fundus background. Thus, green channel image is being used for this part in this project.

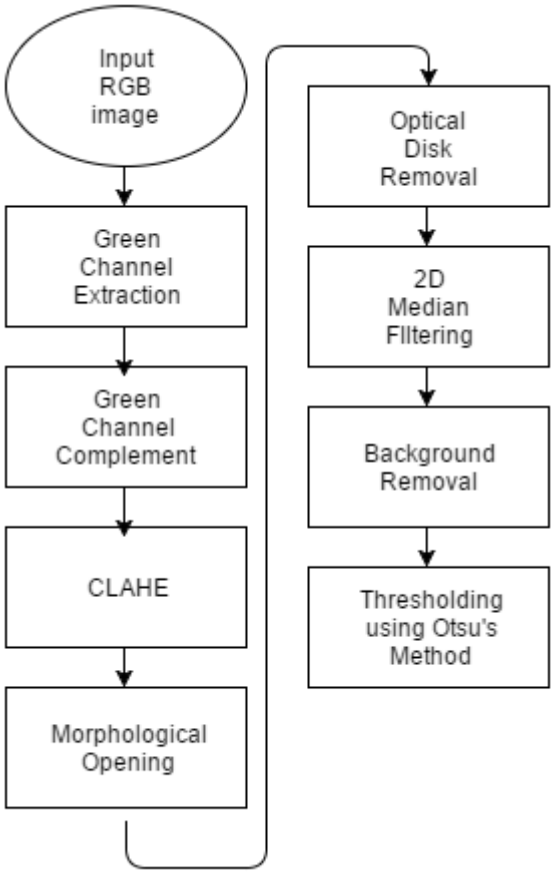


**Figure 3.3.4:** Block diagram for blood vessel masking

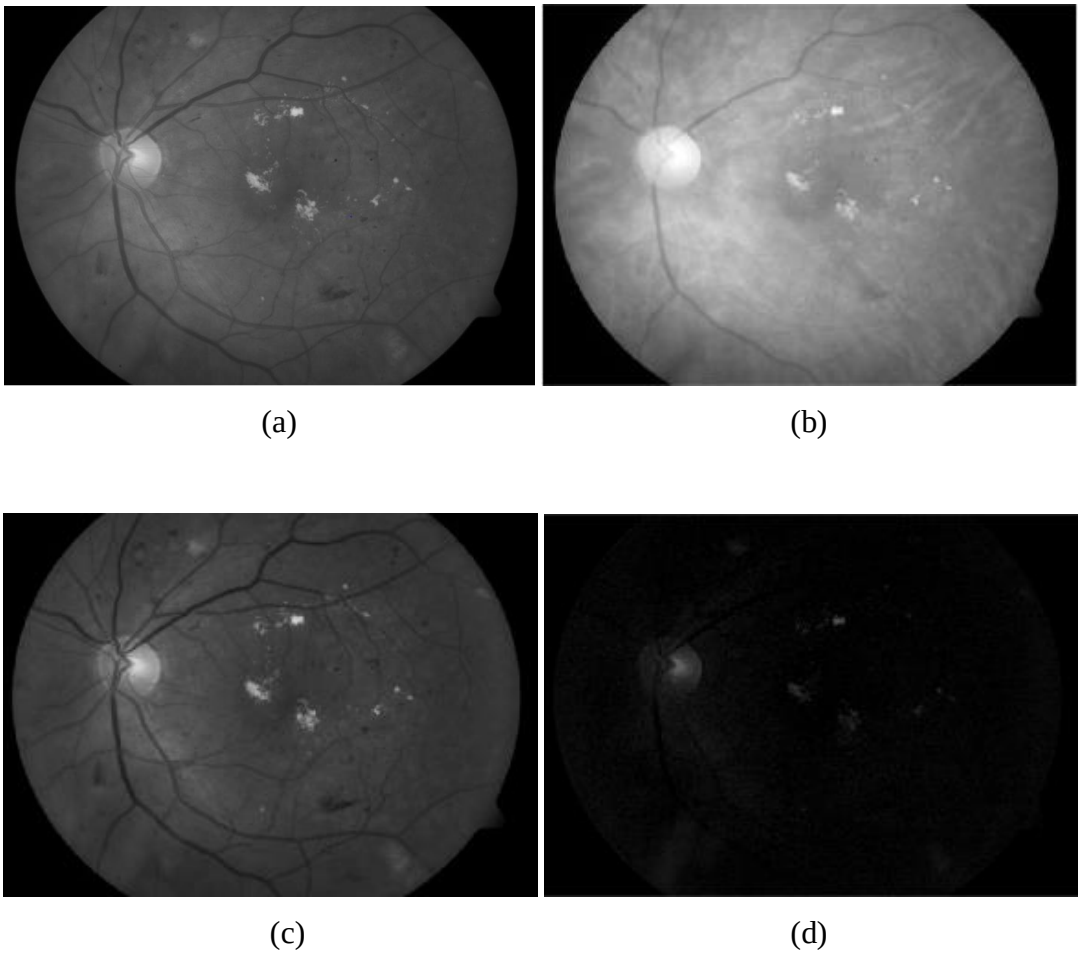

(a) (b)

(c) (d)

**Figure 3.3.5:** Comparison for the clarity of blood vessels network between (a) grayscale image (b) red channel image (c) green channel image (d) blue channel image

Contrast-limited adaptive histogram equalization (CLAHE) is then applied to the complemented Green channel image. CLAHE operates on small regions in the image, called tiles, rather than the entire image. Therefore, this techniques can prevent over amplifying noise in the greyscale image. After that, morphological opening is done to remove white pixel from the image. This section is done to obtain the background image and remove the blood vessels network. This image is than be used again to obtain only the image of the blood vessels without its retinal background by subtracting it with the resultant image of CLAHE. 2-D Median Filtering is then applied to reduce noise of white pixels produced. The then transformed to binary image by performing the Global image threshold using Otsu's method. Lastly the image is complemented to obtain black pixel's

blood vessels network and the image is dilated to ensure full coverage of the blood vessels in the original image later. The overall resultant image for blood vessels masking are shown below.

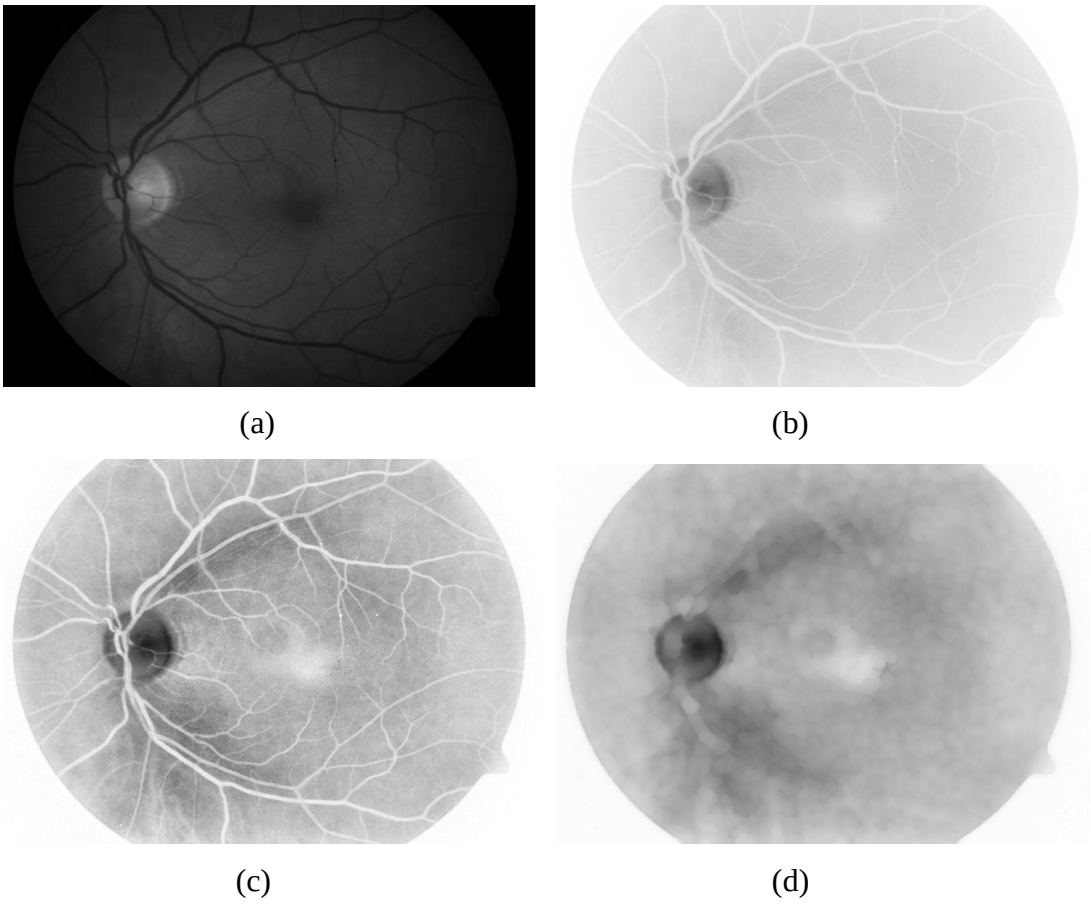

(a) (b)

(c) (d)

**Figure 3.3.6:** Resultant image of every method applied to extract the blood vessels network (a) Green Channel Image (b) Complemented Image (c) CLAHE Operation (d) Morphological Opening

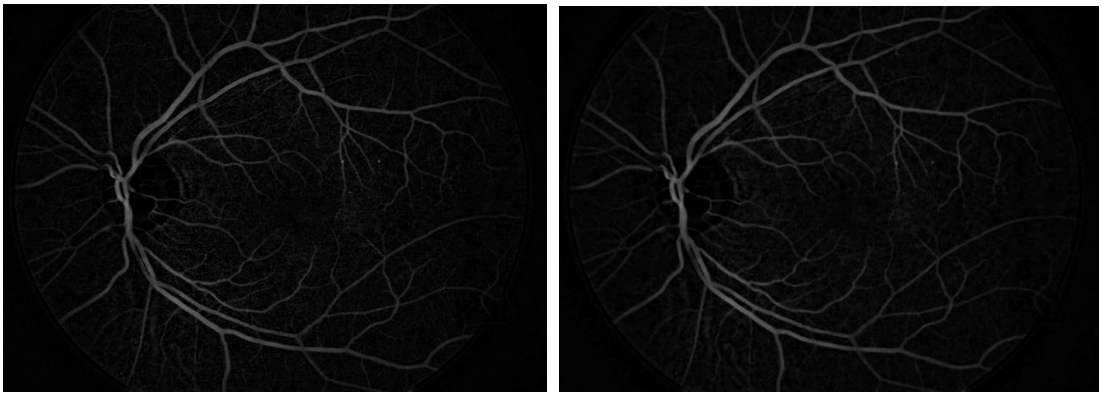

(e) (f)

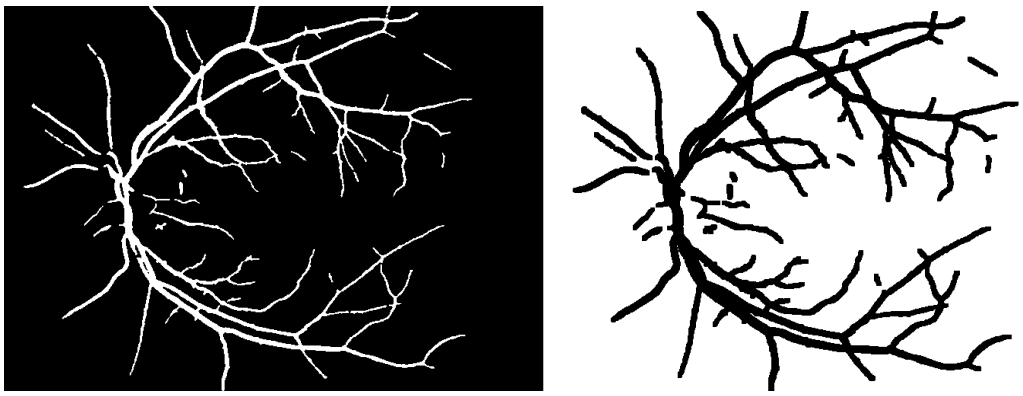

(g) (h)

**Figure 3.3.6:** (e) Background Removed (f) Median Filtering (g) Thresholding (h) Complemented Image

**Binary Mask**

The binary mask that is going to be used for the next phases s formed by multiplying all the masks forming one complete mask. Complete binary mask is shoen in figure 3.3.6.

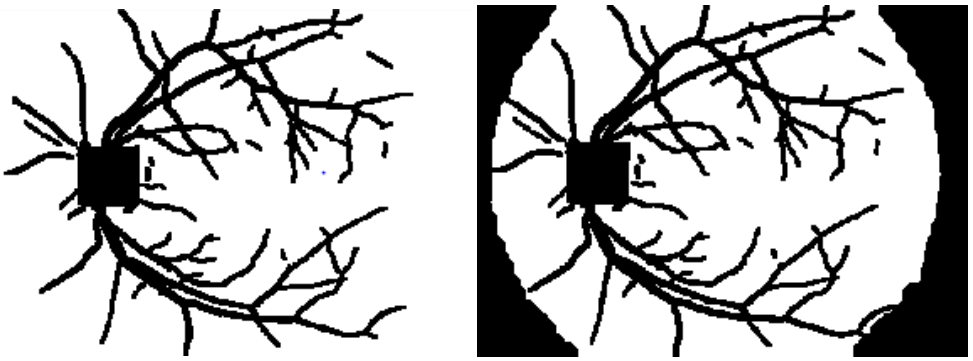

(a) (b)

**Figure 3.3.7:** A complete binary Mask

### 3.3.2 Hemorrhage Enhancement

Hemorrhage are the visible sign of Diabetic Retinopathy (DR) formed in the retina of the eye through blood vessels leakage. They are also known as red lesions and these are the first clinically observable lesions indicating diabetic retinopathy. Therefore, detection of this feature is very important in a diabetic retinopathy screening system.

The major challenges in detecting hemorrhage are:

(i) Segmentation of hemorrhage in low contrast image.

(ii) Presence of anatomical feature generally named Fovea which has same red colour in the middle of the retina.

The principal objective in this phase is to correctly detect the hemorrhage features or dark spots in the retina without mistakenly detecting the blood vessels and low contrast regions in the fundus image.

The proposed hemorrhage enhancement algorithm started with adjusting the hue and saturation value of the colour fundus image in different splitting HSV channel. However, in this method, the intensity value or brightness is left unchanged.

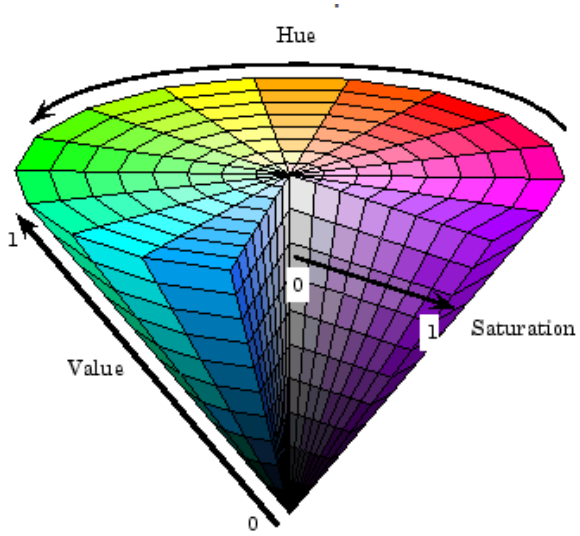


**Figure 3.3.8:** Illustration of HSV colour space (MathWorks 2016)

Hue is expressed as a number from 0 to 360 degrees representing hues of red which start at 0, yellow starting at 60, green starting at 120, cyan starting at 180, blue starting at 240 and magenta starting at 300. However in MATLAB, hue varies from 0 to 1.0, the corresponding colours vary from red through yellow, green, cyan, blue, magenta, and back to red, which means value 0 and 1.0 belongs to red colour (MathWorks 2016). From these six colours, yellow appear to be the best background colour that can help to enhanced red colour of hemorrhage. Therefore, the hue colour is set to match yellow colour.

Saturation is the amount of grey from zero percent to 100 percent in the colour. In MATLAB, saturation varies from 0 to 1.0, the corresponding hue colours then vary from unsaturated with shades of grey on to fully saturated which is no white component left (MathWorks 2016). As hemorrhage features dark spots, the saturation value is set to 1 to remove all possible bright region that could potentially be detected later.

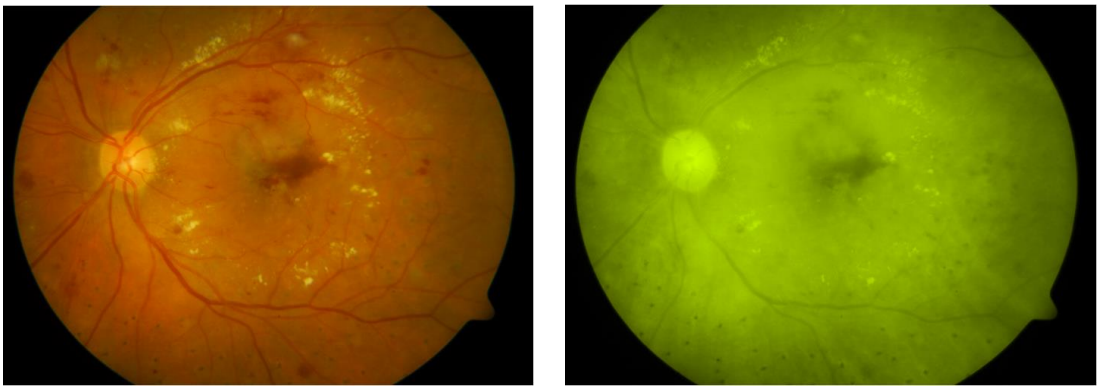

(a) (b)

**Figure 3.3.9:** Enhanced fundus image using HSV adjustment (a) original fundus image (b) HSV adjusted image

### 3.3.3 Feature Extraction of Hemorrhage

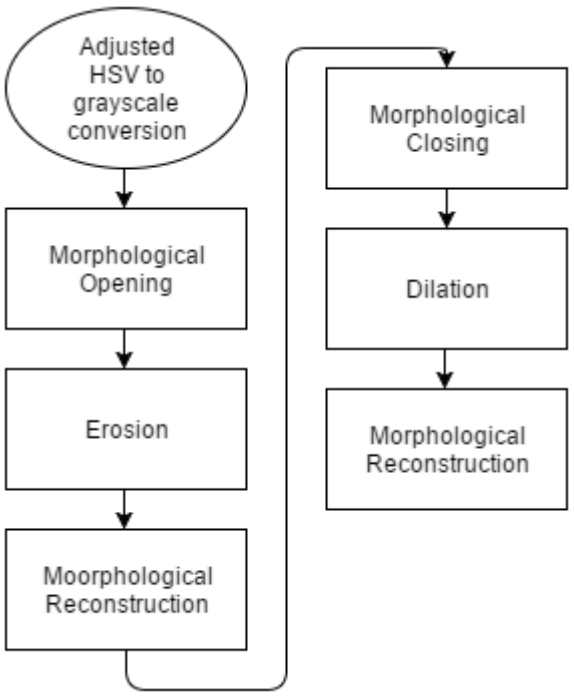


**Figure 3.3.10:** Block diagram for hemorrhage feature extraction

After the image is converted to grayscale, morphological opening operation is performed. Morphological opening is the combination of erosion followed by dilation process. This operation removed some of the foreground bright pixels from the edges of regions of foreground pixels. The process is controlled by a disk – shape structuring element of radius 19. As the result, exudates which has high bright intensity pixel value is removed from the image and the foreground is formed into bright and dark regions. The formulation of morphological opening is as shown below.

$$A \circ B = \cup \{(B)z | (B)z \subseteq A\}$$ (Kamarul HG, Nurul Wahidah A et al. 2016)

Next, erosion is applied to the new resultant image by using the same structuring element to erode away the boundaries of regions of foreground white pixels. The erosion of A by B denoted by $A \ominus B$ is defined as the equation below.

$$A \ominus B = \{z | (B)z \cap A^c \neq \emptyset\}$$ (Kamarul HG, Nurul Wahidah A et al. 2016)

Morphological closing is then applied to the image to enlarge the boundaries of foreground of bright regions in the image. This is to form a smoother resultant image with dark and bright region. Morphological closing is a combination operation of dilation and erosion process. The formulation of morphological closing is defined as below.

$$A \cdot B = (A \oplus B) \ominus B$$ (Kamarul HG, Nurul Wahidah A et al. 2016)

After that, dilation is performed intentionally to enlarge the bright region of the image leaving the dark region to be in smaller regions. This process is done using a new structuring element of disk – shape of smaller radius, which is 5.

Morphological reconstruction is done twice in the hemorrhage feature extraction stage. Morphological reconstruction processes one image, called the marker based on the characteristics of another image, called the mask. The first morphological reconstruction is done after erosion, where the eroded image is reconstruct using imreconstruct function

from MATLAB tools with the grayscale image extracted in the beginning of this stage. In this part, eroded image is the marker while the grayscale image is the mask. The second morphological reconstruction is done after the process of dilation. Here, the first reconstructed image is reconstructed again with complemented dilated image. The first reconstructed image act as the marker while the complemented dilated image act as the mask.

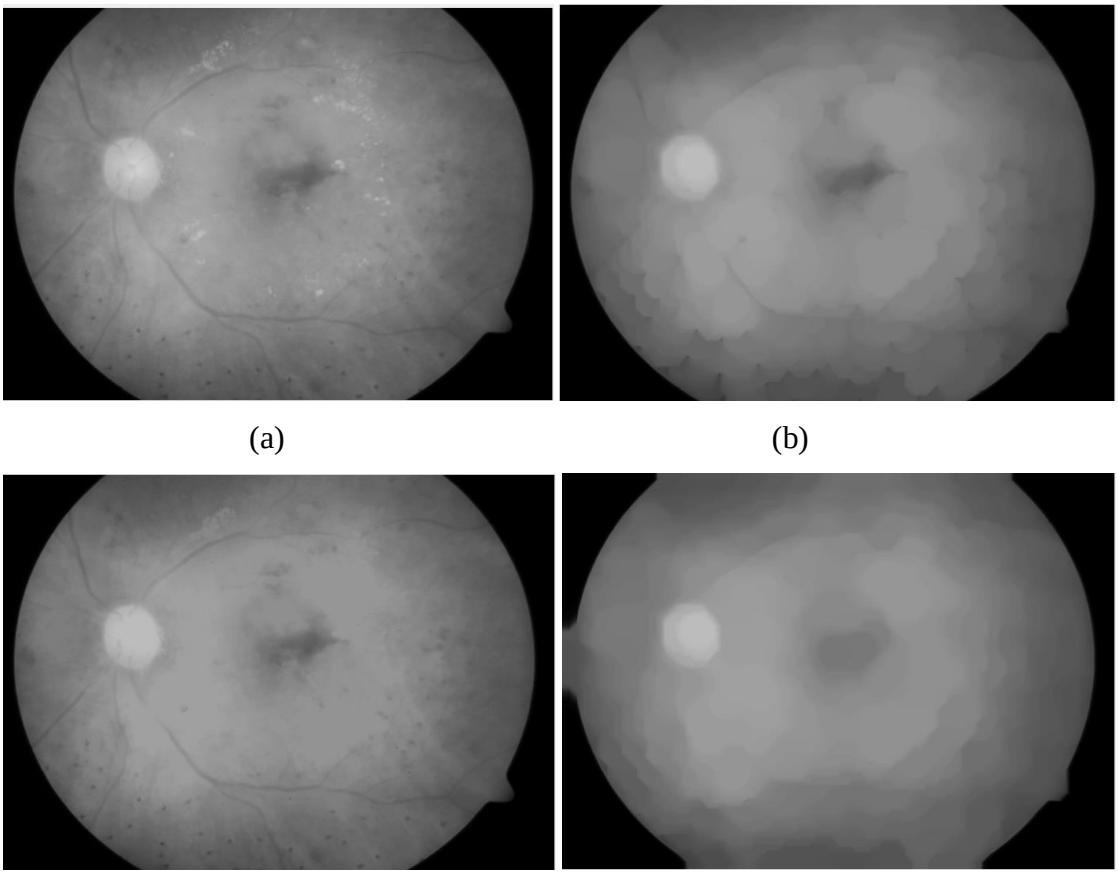

(a) (b)

(c) (d)

**Figure 3.3.11:** Resultant image of every method applied to extract the hemorrhage feature (a) Grayscale Image of Adjusted HSV (b) Morphological Opening (c) Erosion (d) Morphological Closing

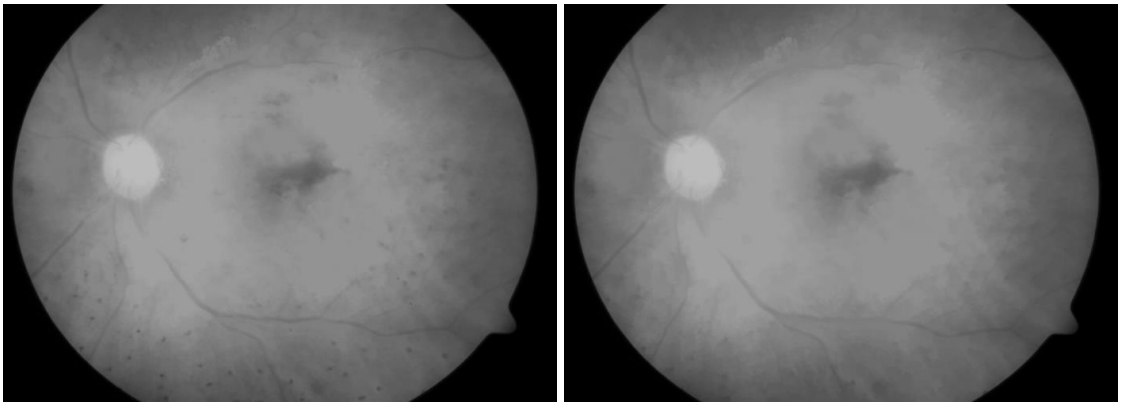

(e) (f)

**Figure 3.3.11:** (d) Morphological Closing (e) Dilation (f) Restructure

### 3.3.4 Decision Making for Hemorrhage Detection

For the decision making, regional minima from MATLAB toolbox is used to extract only the small regions which is mainly the dark regions. Regional minima are connected components of pixels with a constant intensity value obtained from the previous operations, and whose external boundary pixels all have a higher value (MathWorks 2016). In BW, pixels that are set to 1 identify regional minima all other pixels are set to 0. Lastly, the output image is masked to ensure that no blood vessels spots come in existence with the extracted hemorrhage feature. Process for marking out the haemorrhage is shown in figure 3.3.10.

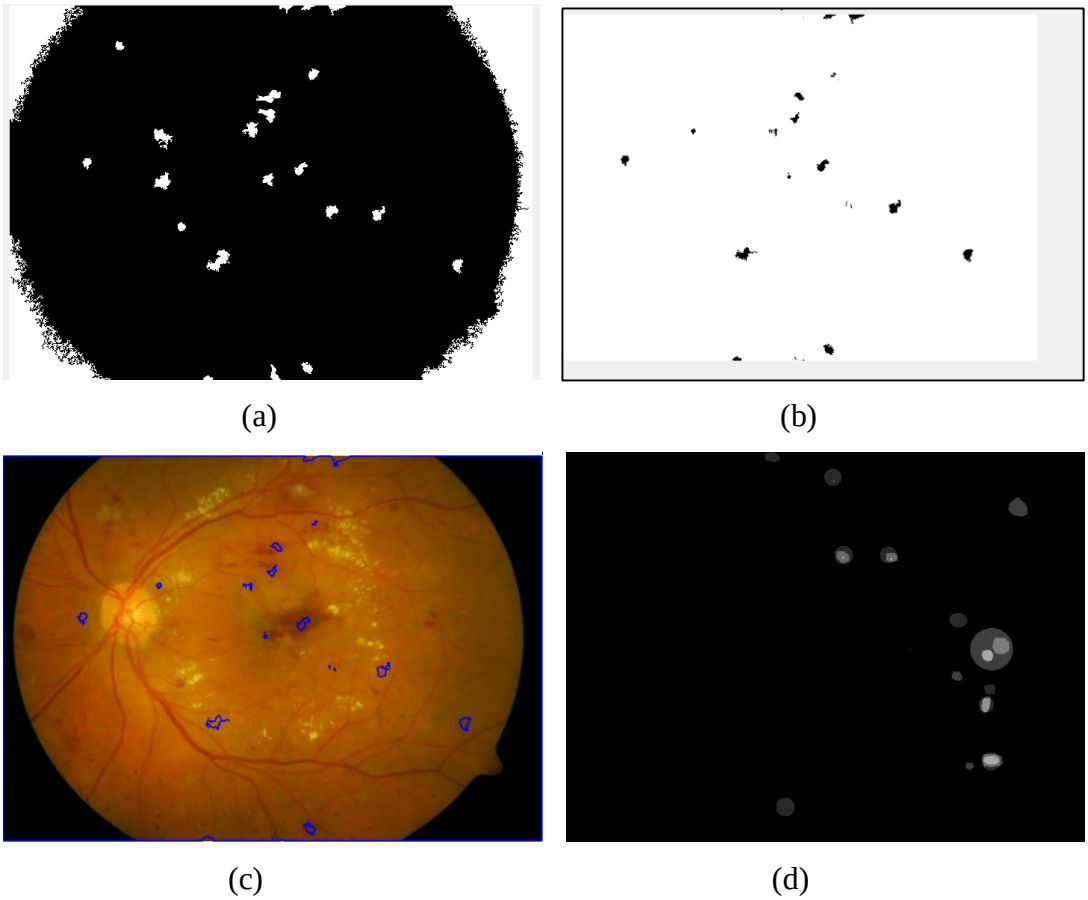

(a) (b)

(c) (d)

**Figure 3.3.12:** Process for marking out the hemorrhage (a) Regional Minima (b) Masked Regional Minima (c) Marked hemorrhage on original fundus image (d) Ground truth image

## 3.4 EXUDATES DETECTION ALGORITHM

### 3.4.1 Optic Disk, Retinal Background and Blood Vessel Removal

The method for optic disk, background and blood vessels removal in this part is as the same as previous method. The same mask is being used in both hemorrhage and exudates detection due to its respective images.

### 3.4.2 Exudates Enhancement

Exudates can be view as bright patterns in colour fundus images of the human retina and they are very well contrasted with respect to their surrounding background. Their shape and size vary considerably and their borders are mostly irregular. However, there is problem with detecting exudates in low contrast fundus image. Presence of small black dots giving the image a sharp edges that could be mistakenly detected as exudates.

The main purpose of this phase is to extract the exudates feature and distinguish it from optical disk. Suppose optical disk is not a problem anymore because masking of this anatomical feature had been done in earlier stage. The optical disk is now can be considered as black colour. Therefore the solution for image enhancement, the fundus image is converted to green channel as green channel provides high contrast between the exudates and the fundus background. Figure below shows the comparison of grayscale image and spitted RGB channel images of red channel, green channel and blue channel.

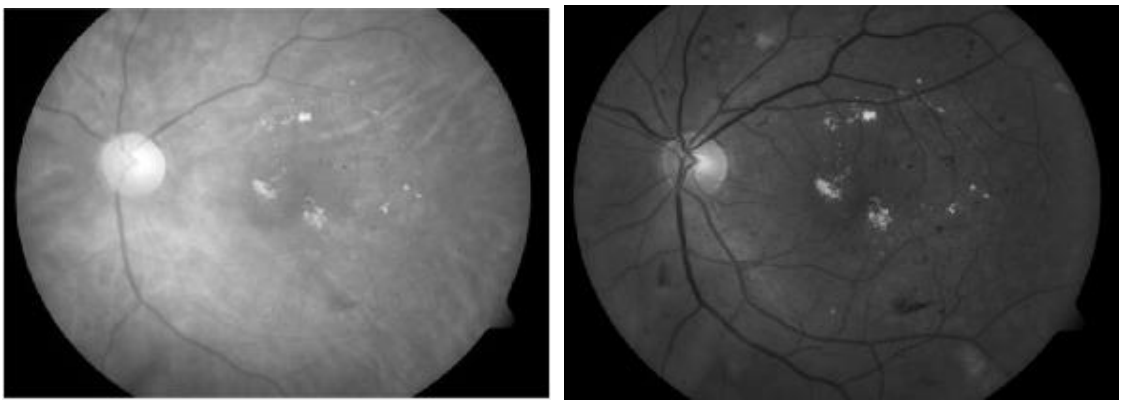

(a) (b)

**Figure 3.4.1:** Comparison for exudates clarity in (a) Red Channel Image (b) Green Channel Image

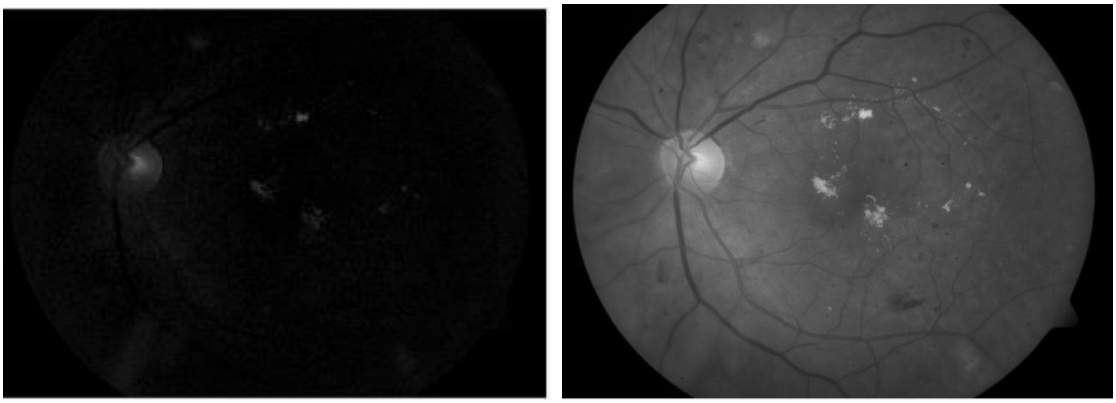

(c) (d)

**Figure 3.4.1:** (c) Blue Channel Image (d) Grayscale Image

### 3.4.3 Feature Extraction of Exudates

For feature extraction, predefined 2-D filter is created using Prewitt horizontal edge-emphasizing filter. Prewitt filter is the gradient – based algorithm that calculates the gradient of the image intensity at each point, giving the direction of the largest possible increase from light to dark pixel. The result of gradient magnitude therefore shows the detected edge of the features of different pixel intensities. The output images from this method can be seen on the figure 3.4.2.

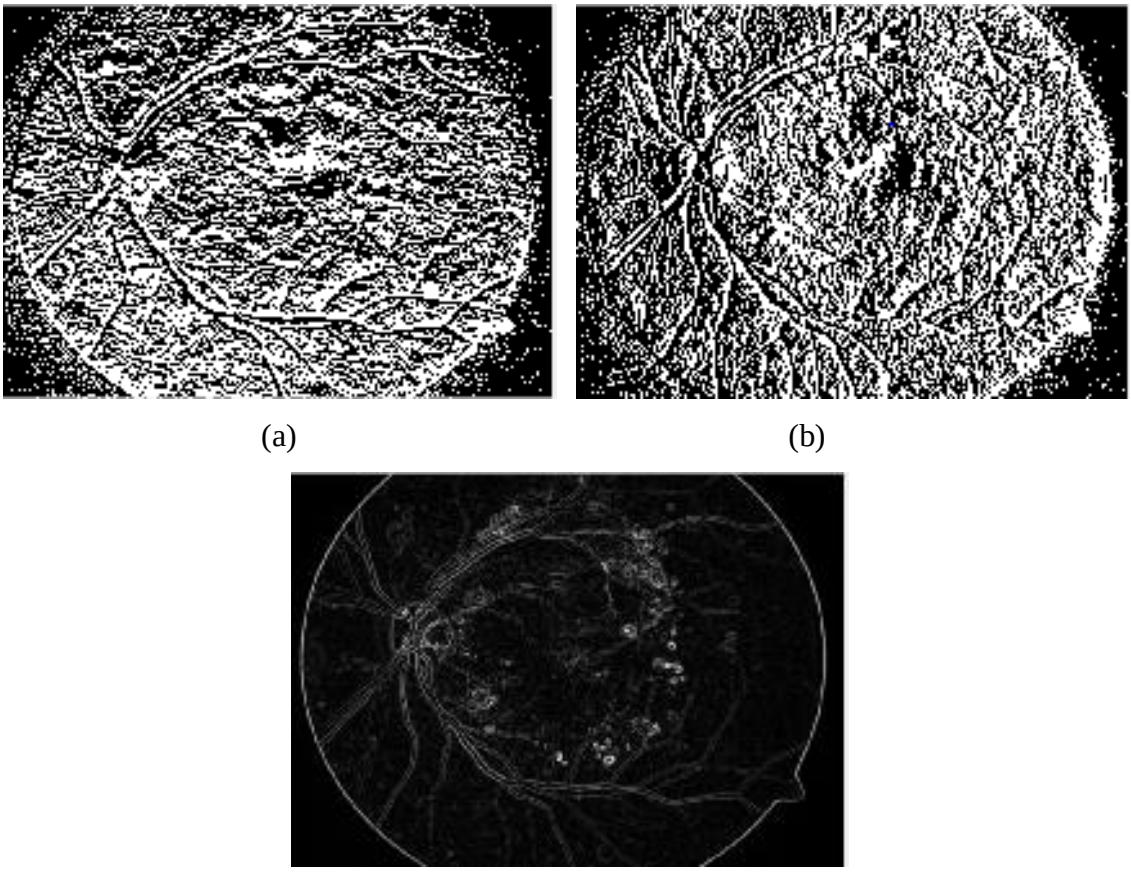

(a) (b)

(c)

**Figure 3.4.2:** Exudates feature extraction (a) 1st derivative of Prewitt filter (b) 2nd derivative of Prewitt filter (c) Gradient Magnitude

### 3.4.4 Decision Making for Exudates Detection

After masking, region of interest (ROI) pixel selection is done by setting the possible minimum to maximum pixel value of exudates. To do this, all 89 sample images is processed and then the pixel value range is listed to find the most perfect minimum and maximum exudates' pixel value range. The minimum pixel is set to 70 while the maximum pixel value is set to 155. The output image then shows extracted exudates features.

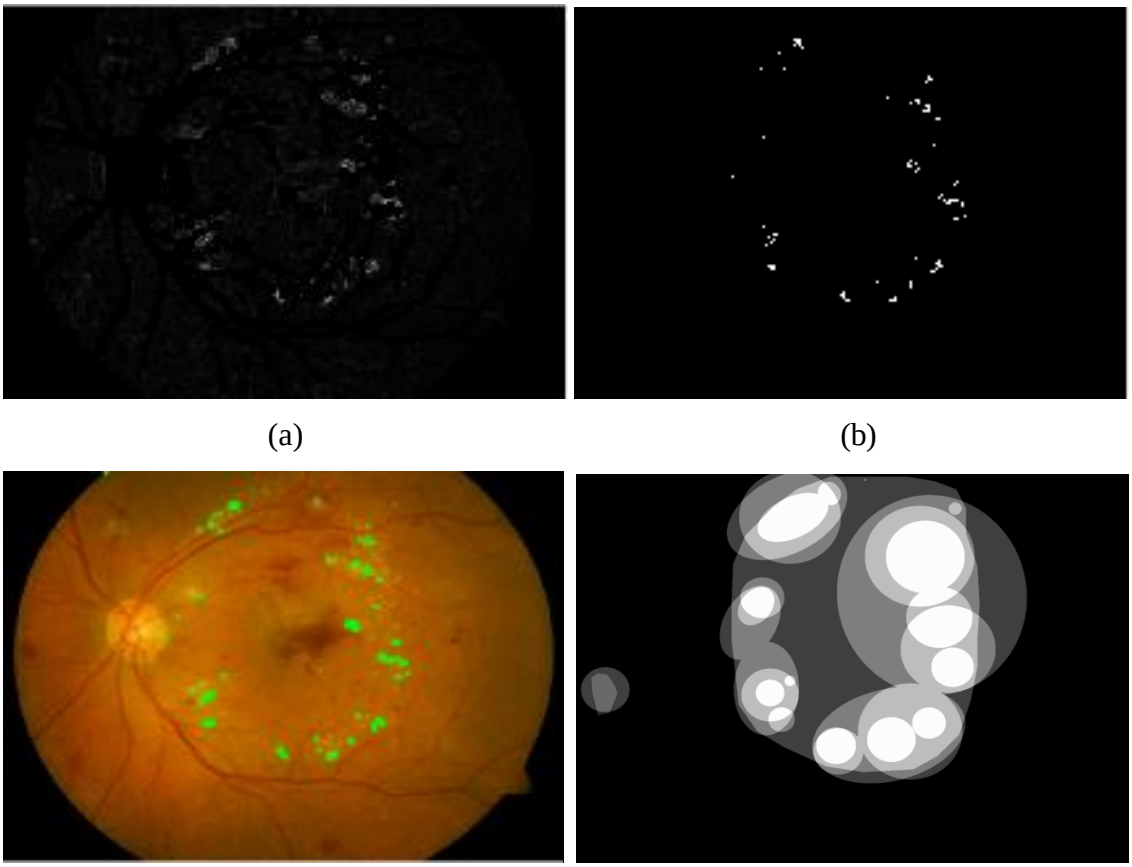

(a) (b)

(c) (d)

**Figure 3.4.3:** Process for marking out the exudates (a) Masked Gradient Magnitude (b) ROI selection (c) Marked exudates on original fundus image (d) Ground truth image

# CHAPTER 4

# RESULTS AND DISCUSSIONS

## 4.1 INTRODUCTION

In this thesis, several screening system components are developed including blood vessel segmentation, localization and contour detection of optic disk, hemorrhage extraction and exudates extraction. In this chapter these components are combined in a form of graphical user interface using MATLAB Graphical User Interface Development Environment (GUIDE) to form a complete Fundus Image Analysis (FIA) system that can be employed for diabetic retinopathy screening. The system starts by manually selecting the optical disk using ROIPOLY toolbox and then automatically segmenting the blood vessels to form a complete binary mask. Next, hemorrhage and exudates are extracted and marked in the fundus image.

## 4.2 GRAPHICAL USER INTERFACE

Graphical User Interface (GUI) is developed as an interactive tools for clinicians to use. GUI that provides user friendly interface makes the system easier to operate compared to basic MATLAB coding form.

The developed GUI consist of a few operational button including the *Load Image* button, *Masking* button, *Hemorrhage Detection* button, *Exudates Detection* button and *Reset* button. The designed GUI is as shown in figure 4.1 below.

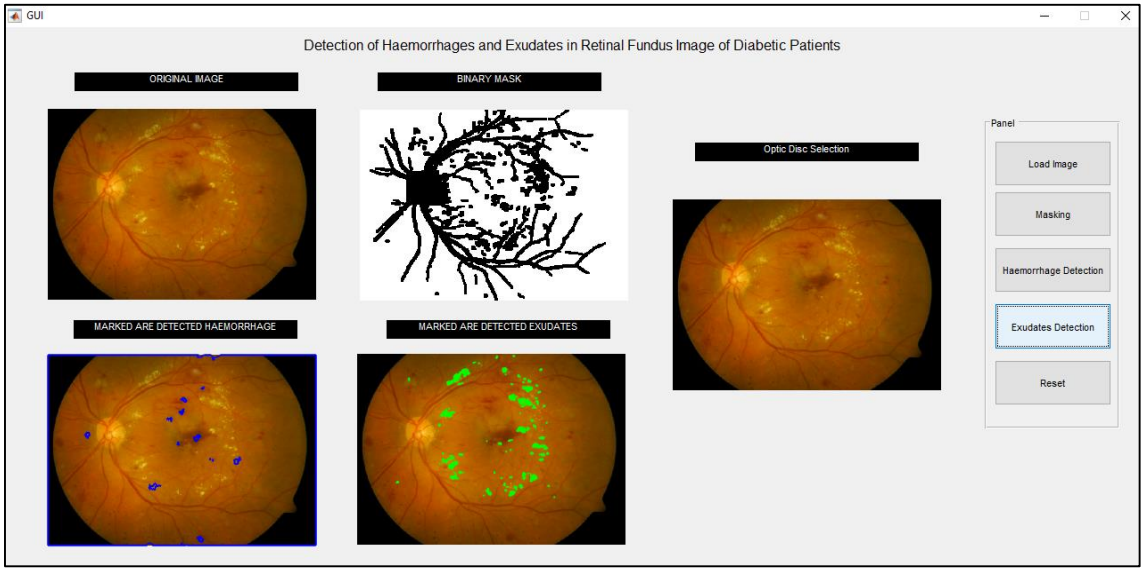


**Figure 4.1:** Developed Graphical User Interface (GUI)

Function for each buttons are:

(i) Load button – load button let user choose any captured retinal fundus image from a file.

(ii) Masking button – this button starts with a pop – up figure that asked user to manually select the optical disk of the loaded image. After selection is done, a complete binary mask will appear in it corresponding figure space.

(iii) Hemorrhage Detection button – by clicking this button, a processed image with hemorrhage features marked in blue colour will appear in it corresponding figure space.

(iv) Exudates Detection button – by clicking this button, a processed image with exudates features marked in green colour will appear in it corresponding figure space.

(v) Reset button – this button let user clear out all figure spaces before loading a new image.

## 4.3 PERFORMANCE STUDY

The performance of the developed system is studied by comparing the output image of all 89 sample images with the ground truth provided by the Standard Diabetic Retinopathy Database (DIARETDB1). The purpose of this study is to determine the accuracy of the proposed algorithm for this system. To compare the output result with the provided ground truth, an input fundus image need to complete all the phases in the developed Fundus Image Analysis (FIA) system starting with masking phase, hemorrhage detection phase and exudates detection phase. Figure 4.2 shows an example of fundus image through all complete phases.

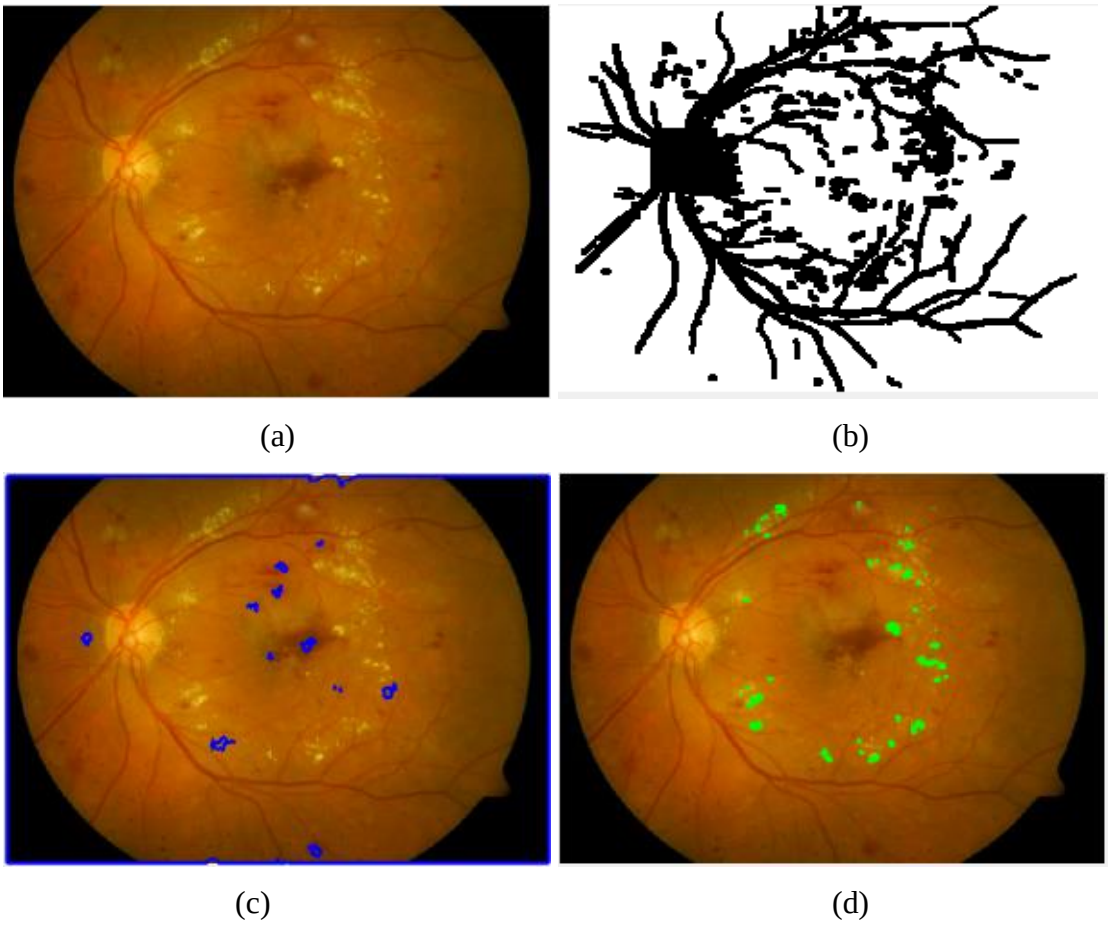

(a) (b)

(c) (d)

**Figure 4.2:** Complete phases of the developed FIA system (a) Input Fundus Image (b) Masking Phase (c) Hemorrhage Detection Phase (d) Exudates Detection Phase

After the result for hemorrhage detection and exudates detection is obtained for all 89 sample images, these results is then compared with provided ground truth so that the accuracy of the system can be calculated. Figure 4.3 shows a few resultant image extracted by the system which are successfully matched the ground truth while figure 4.4 shows examples of resultant image that are unsuccessful to match the given ground truth.

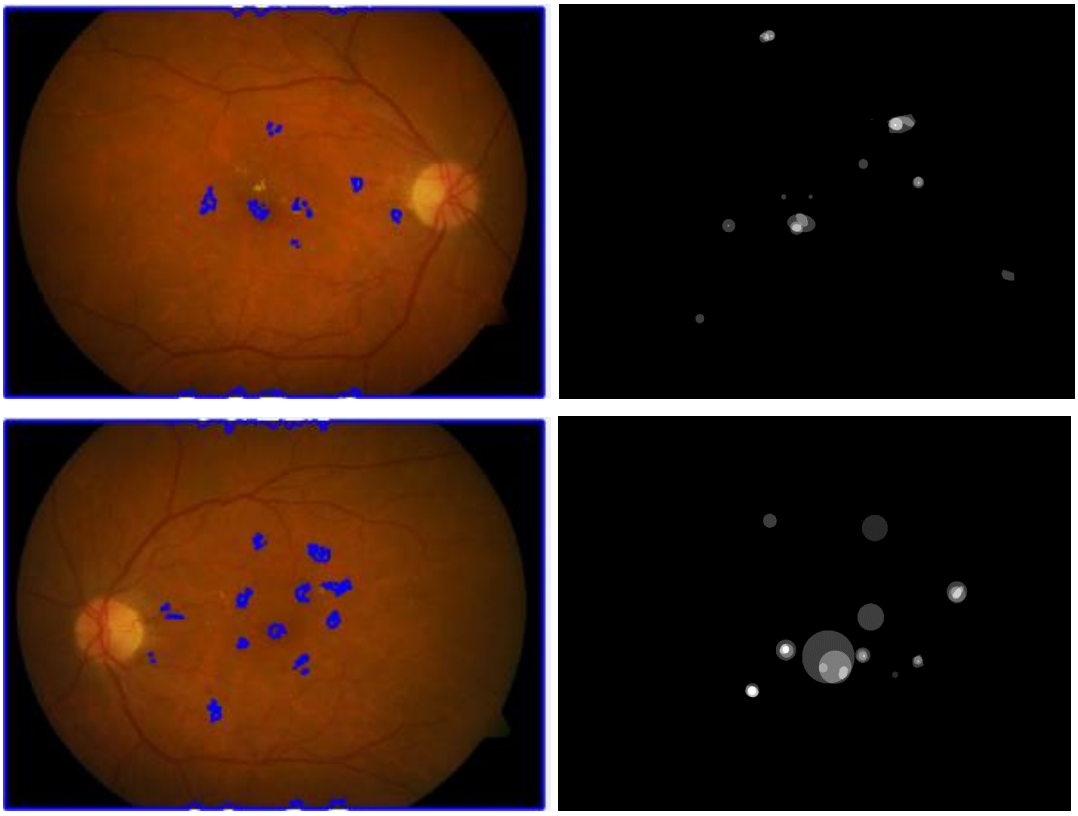

(a)

**Figure 4.3:** Successful features detection as compared to its ground truth (a) hemorrhage detection [left image is the resultant image from FIA system. Right image is the ground truth]

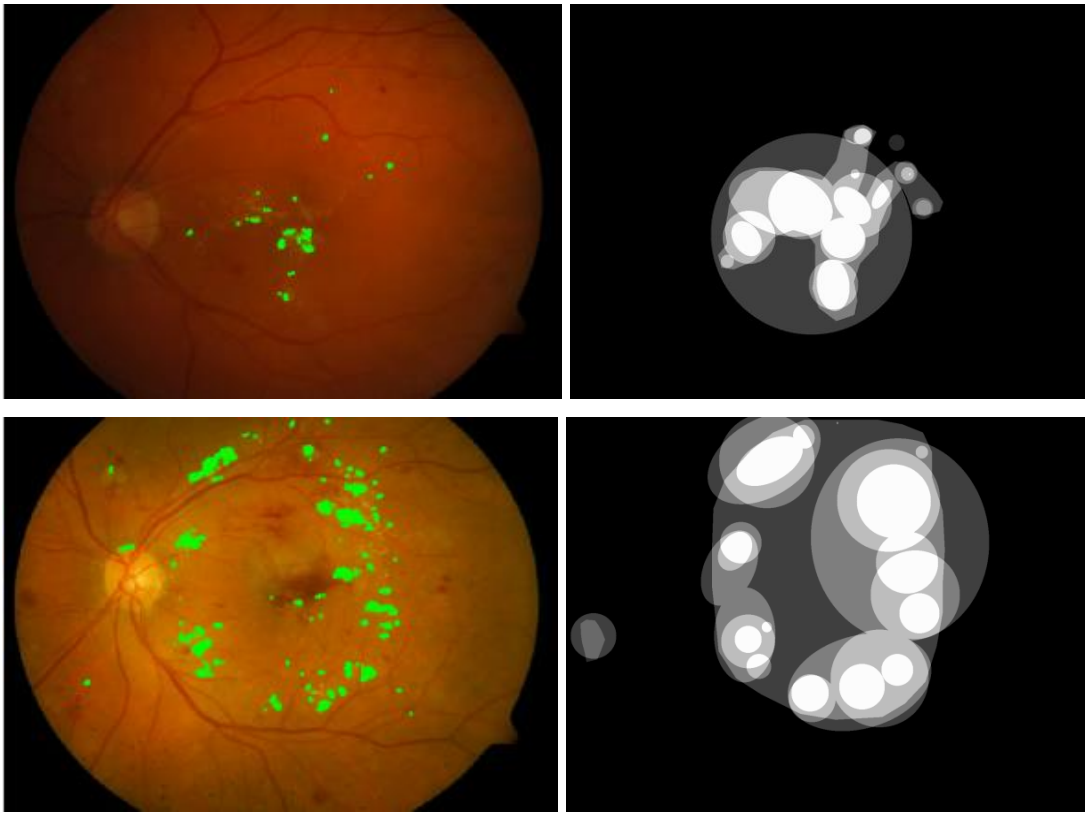

(b)

**Figure 4.3:** Successful features detection as compared to its ground truth (b) exudates detection [left image is the resultant image from FIA system. Right image is the ground truth]

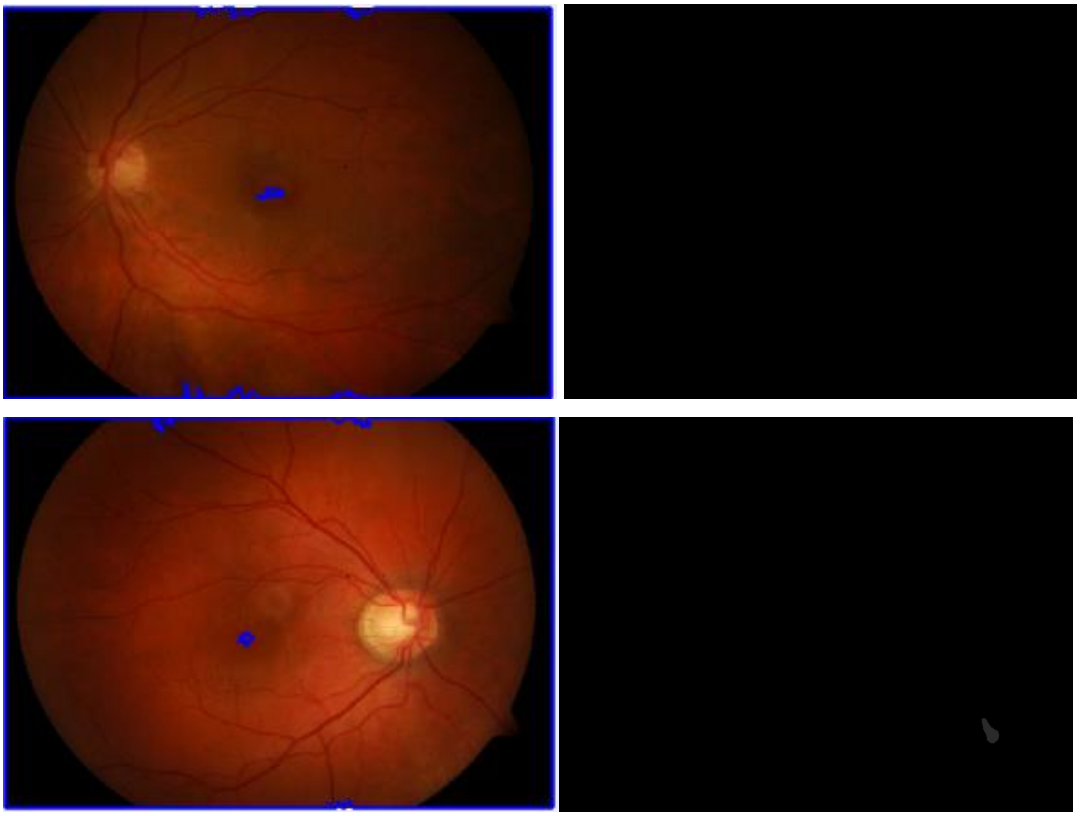

(a)

**Figure 4.4:** Unuccessful features detection as compared to its ground truth (a) hemorrhage detection [left image is the resultant image from FIA system. Right image is the ground truth]

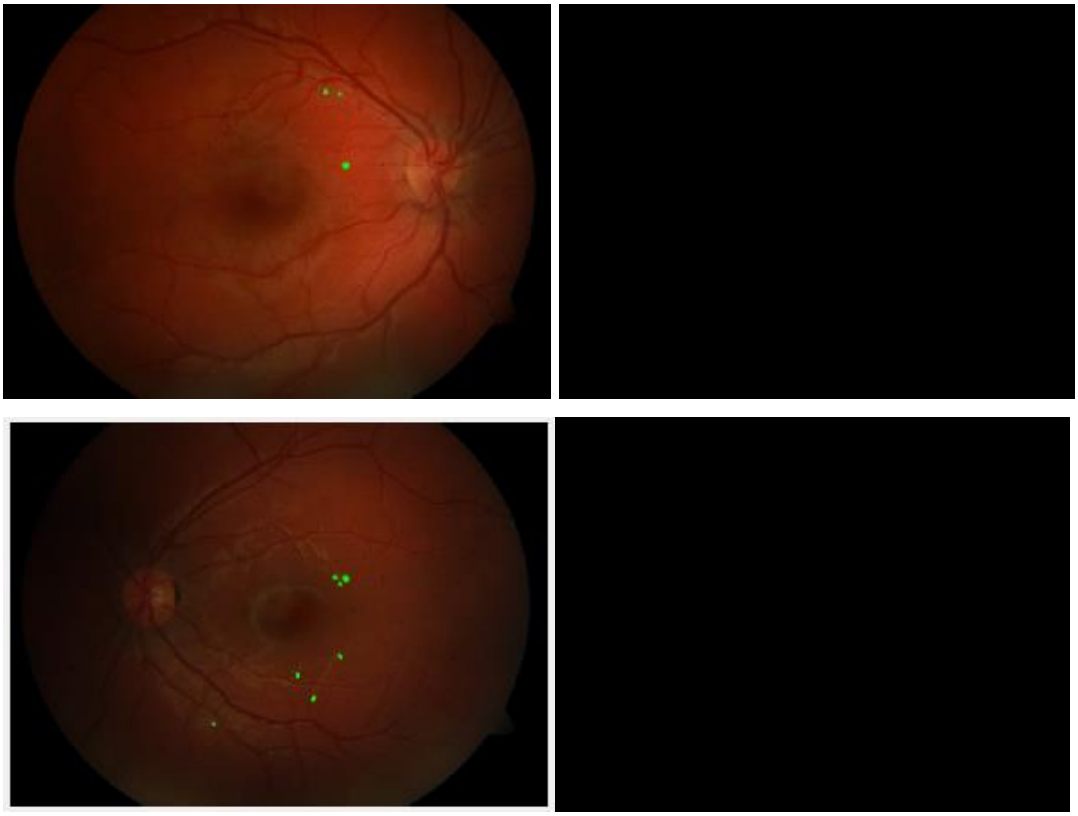

(b)

**Figure 4.4:** (b) exudates detection [left image is the resultant image from FIA system. Right image is the ground truth]

Table 4.3 is constructed to visualize the successfulness of the system in determining haemorrhage and exudates features in correspond to each sample fundus images. The images that are successfully extract corresponding features are marked green while unsuccessful images are marked red.

**Table 4.3:** Successfulness data for every images

| Image Number | Hemorrhage | Exudates |
|---|---|---|
| Image001 | **Successful** | **Successful** |
| Image002 | **Successful** | **Successful** |
| Image003 | **Successful** | **Successful** |
| Image004 | **Successful** | **Successful** |
| Image005 | **Successful** | **Successful** |
| Image006 | **Successful** | **Successful** |
| Image007 | **Successful** | **Successful** |
| Image008 | **Successful** | **Successful** |
| Image009 | **Successful** | **Successful** |
| Image010 | **Successful** | **Successful** |
| Image011 | **Successful** | **Successful** |
| Image012 | **Successful** | **Successful** |
| Image013 | **Successful** | **Successful** |
| Image014 | **Successful** | **Successful** |
| Image015 | **Successful** | **Successful** |
| Image016 | **Successful** | **Successful** |
| Image017 | **Successful** | **Successful** |
| Image018 | **Successful** | **Successful** |
| Image019 | **Successful** | **Successful** |
| Image020 | **Successful** | **Successful** |
| Image021 | **Successful** | **Successful** |
| Image022 | **Successful** | **Successful** |
| Image023 | **Unsuccessful** | **Unsuccessful** |
| Image024 | **Unsuccessful** | **Successful** |
| Image025 | **Successful** | **Successful** |
| Image026 | **Successful** | **Successful** |
| Image027 | **Unsuccessful** | **Unsuccessful** |

| | | |
|---|---|---|
| Image028 | **Unsuccessful** | **Unsuccessful** |
| Image029 | **Unsuccessful** | **Unsuccessful** |
| Image030 | **Unsuccessful** | **Successful** |
| Image031 | **Unsuccessful** | **Successful** |
| Image032 | **Unsuccessful** | **Successful** |
| Image033 | **Unsuccessful** | **Successful** |
| Image034 | **Unsuccessful** | **Successful** |
| Image035 | **Successful** | **Successful** |
| Image036 | **Unsuccessful** | **Unsuccessful** |
| Image037 | **Unsuccessful** | **Unsuccessful** |
| Image038 | **Unsuccessful** | **Successful** |
| Image039 | **Unsuccessful** | **Successful** |
| Image040 | **Unsuccessful** | **Unsuccessful** |
| Image041 | **Successful** | **Unsuccessful** |
| Image042 | **Unsuccessful** | **Successful** |
| Image043 | **Successful** | **Unsuccessful** |
| Image044 | **Unsuccessful** | **Successful** |
| Image045 | **Unsuccessful** | **Unsuccessful** |
| Image046 | **Unsuccessful** | **Successful** |
| Image047 | **Unsuccessful** | **Unsuccessful** |
| Image048 | **Unsuccessful** | **Unsuccessful** |
| Image049 | **Unsuccessful** | **Unsuccessful** |
| Image050 | **Unsuccessful** | **Unsuccessful** |
| Image051 | **Unsuccessful** | **Unsuccessful** |
| Image052 | **Successful** | **Successful** |
| Image053 | **Successful** | **Successful** |
| Image054 | **Successful** | **Successful** |
| Image055 | **Unsuccessful** | **Successful** |
| Image056 | **Unsuccessful** | **Unsuccessful** |
| Image057 | **Unsuccessful** | **Unsuccessful** |

| | | |
|---|---|---|
| Image058 | **Successful** | **Unsuccessful** |
| Image059 | **Unsuccessful** | **Successful** |
| Image060 | **Unsuccessful** | **Unsuccessful** |
| Image061 | **Unsuccessful** | **Unsuccessful** |
| Image062 | **Unsuccessful** | **Successful** |
| Image063 | **Unsuccessful** | **Unsuccessful** |
| Image064 | **Successful** | **Successful** |
| Image065 | **Successful** | **Unsuccessful** |
| Image066 | **Successful** | **Successful** |
| Image067 | **Successful** | **Successful** |
| Image068 | **Unsuccessful** | **Successful** |
| Image069 | **Unsuccessful** | **Successful** |
| Image070 | **Unsuccessful** | **Successful** |
| Image071 | **Unsuccessful** | **Successful** |
| Image072 | **Unsuccessful** | **Unsuccessful** |
| Image073 | **Unsuccessful** | **Unsuccessful** |
| Image074 | **Unsuccessful** | **Unsuccessful** |
| Image075 | **Unsuccessful** | **Successful** |
| Image076 | **Unsuccessful** | **Successful** |
| Image077 | **Unsuccessful** | **Successful** |
| Image078 | **Unsuccessful** | **Successful** |
| Image079 | **Unsuccessful** | **Successful** |
| Image080 | **Unsuccessful** | **Successful** |
| Image081 | **Unsuccessful** | **Successful** |
| Image082 | **Unsuccessful** | **Successful** |
| Image083 | **Unsuccessful** | **Successful** |
| Image084 | **Successful** | **Successful** |
| Image085 | **Successful** | **Successful** |
| Image086 | **Unsuccessful** | **Successful** |
| Image087 | **Unsuccessful** | **Unsuccessful** |

| | | |
|---|---|---|
| Image088 | **Unsuccessful** | **Unsuccessful** |
| Image089 | **Unsuccessful** | **Unsuccessful** |

**Evaluation Results and Discussion**

The database sample image consist of 89 fundus images with combinations of haemorrhage and exudates features. After sorting out the images based on the ground truth provided, it can be generalize that from the 89 images, 52 of the images are defected with haemorrhage while 37 of the images are not defected with hemorrhage. As for exudates, 43 of the images are defected with exudates while 46 of them are not defected.

**Table 4.4:** Number of Defected and Non – Defected Images

| Features | Defected | Non – Defected |
|---|---|---|
| Hemorrhage | 52 | 37 |
| Exudates | 43 | 46 |

A dataset of 89 sample fundus images is used for assessing the proposed Fundus Image Analysis (FIA) system. The images acquired from the public database consist of diverse quality of image in term brightness and lucidity. The images in these databases are classified as normal and abnormal based on the presence and absence of the hemorrhage and exudates. The DIRETDB1 comprises 60 abnormal images and 29 normal images. However, by using the developed system, the abnormal features is detected in 74 images out of 89 images.

The earlier performance study shows that the developed system does generate false result to some images where some features are not correctly detected or unable to be detected. Therefore, confusion matrix for the system is tabulated for accuracy analysis.

**Hemorrhage Analysis**

Defected = Image with hemorrhage

Non – Defected = Image without hemorrhage

**Table 4.5:** Hemorrhage Confusion Matrix

| | | PREDICTED | |
|---|---|---|---|
| | | Defected | Non – Defected |
| ACTUAL | Defected | 43 | 9 |
| | Non – Defected | 37 | 0 |

From the confusion matrix, the following information is extracted. Table 4.2.6 shows the corresponding table of confusion for haemorrhage class.

**Table 4.6:** Outcome from Hemorrhage Class

| | |
|---|---|
| True Positive (TP)<br>(actual defected image that were correctly classified as defected) | 43 |
| False Negative (FN)<br>(defected images that were incorrectly marked as non – defected images) | 9 |
| False Positive (FP)<br>(non – defected images that were incorrectly labelled as defected images) | 37 |
| True Negative (TN)<br>(all the remaining images, correctly classified as non – defected images) | 0 |

**Sensitivity, Specificity & Accuracy**

$$Sensitivity = \frac{\mathrm{TP}}{\mathrm{TP} + \mathrm{FN}}$$

$$Specificity = \frac{\mathrm{TN}}{\mathrm{FP} + \mathrm{TN}}$$

$$accuracy = \frac{\mathrm{TP}}{(\mathrm{TP} + \mathrm{FN}) + \mathrm{FP} + \mathrm{TN}}$$

To find the accuracy for the developed system, calculation is made based on the defected images.

$$Sensitivity = \frac{\mathrm{TP}}{\mathrm{TP} + \mathrm{FN}}$$
$$= \frac{43}{43 + 9}$$
$$= 0.8269$$
$$= 82.69\%$$

$$Specificity = \frac{\mathrm{TN}}{\mathrm{FT} + \mathrm{TN}}$$
$$= \frac{0}{37 + 0}$$
$$= 0.0000$$
$$= 0.00\%$$

$$Accuracy = \frac{\mathrm{TP} + \mathrm{TN}}{(\mathrm{TP} + \mathrm{FN}) + (\mathrm{FP} + \mathrm{TN})}$$
$$= \frac{43 + 0}{(43 + 9) + (37 + 0)}$$
$$= 0.4831$$
$$= 48.31\%$$

The presence of hemorrhage is poorly detected by the FIA system in all 89 images with the sensitivity of 82.69% and specificity of 0.00%. Specificity is the measure of proportion for defective image that are correctly identified as defective images. Extraction of hemorrhage has 0.00% specificity due to false

detection of an anatomical feature named fovea. The fovea is a small, central pit composed of closely packed cones in the eye. It is located in the centre of the macula of the retina. Figure 4.5 shows the example of detected fovea that lead to high false positive result.

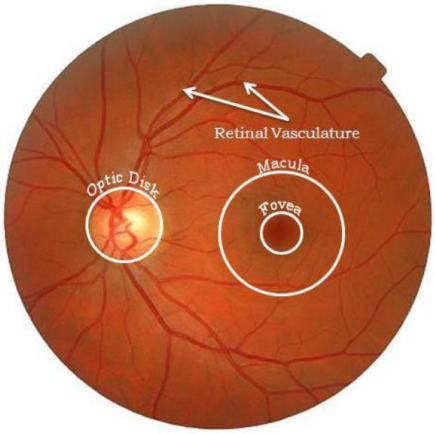


(a)

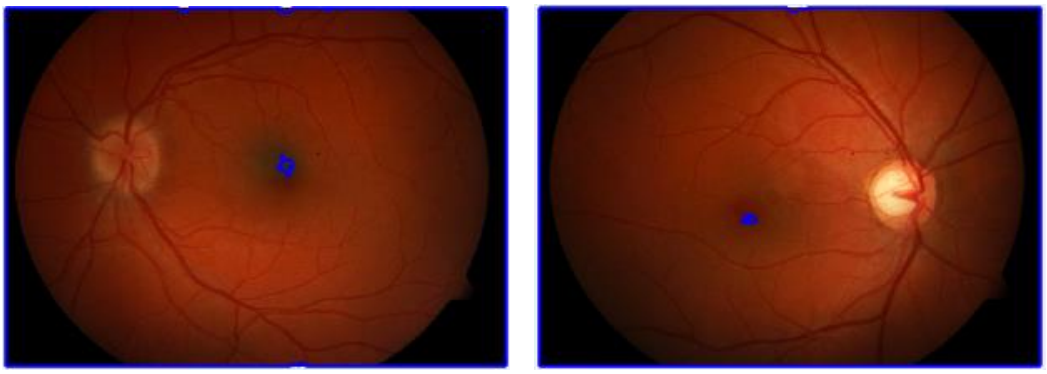

(b)

**Figure 4.5:** False positive detection of fovea example images (a) Fovea Diagram (b) Examples Of False Positive Detection Images

In this system, the fovea is hard to be distinguished from hemorrhage because both of the features has a closely approximate pixel value. Figure 4.6 below shows the pixel value of hemorrhage and fovea in grayscale image. From here, it can be observed that the pixel value for both fovea and hemorrhage is in the range of 0.3.

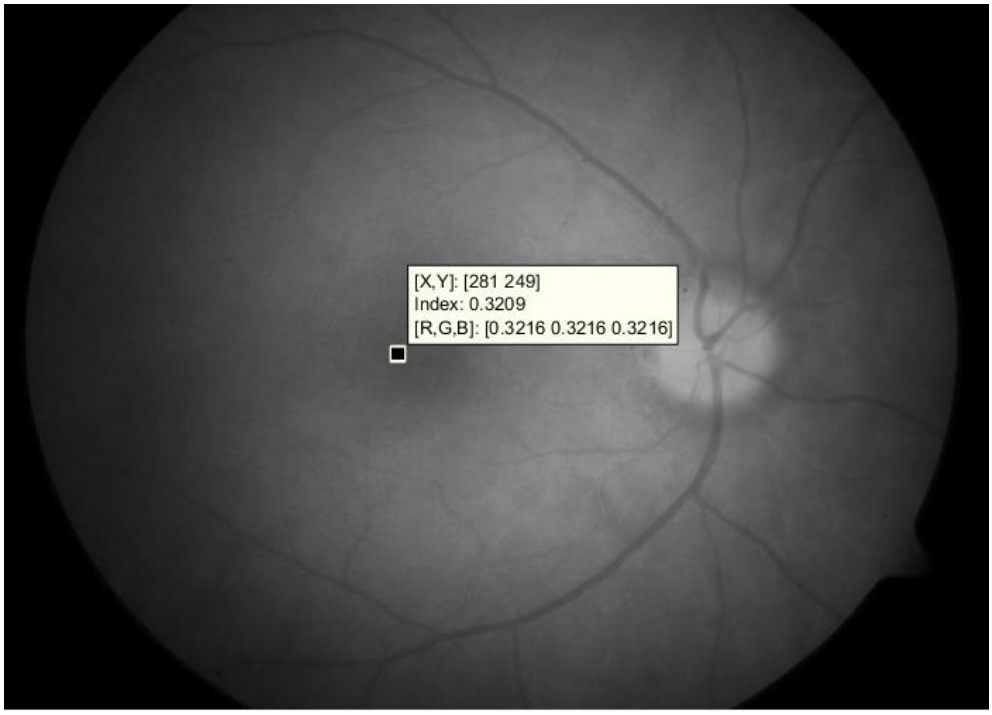


(a)

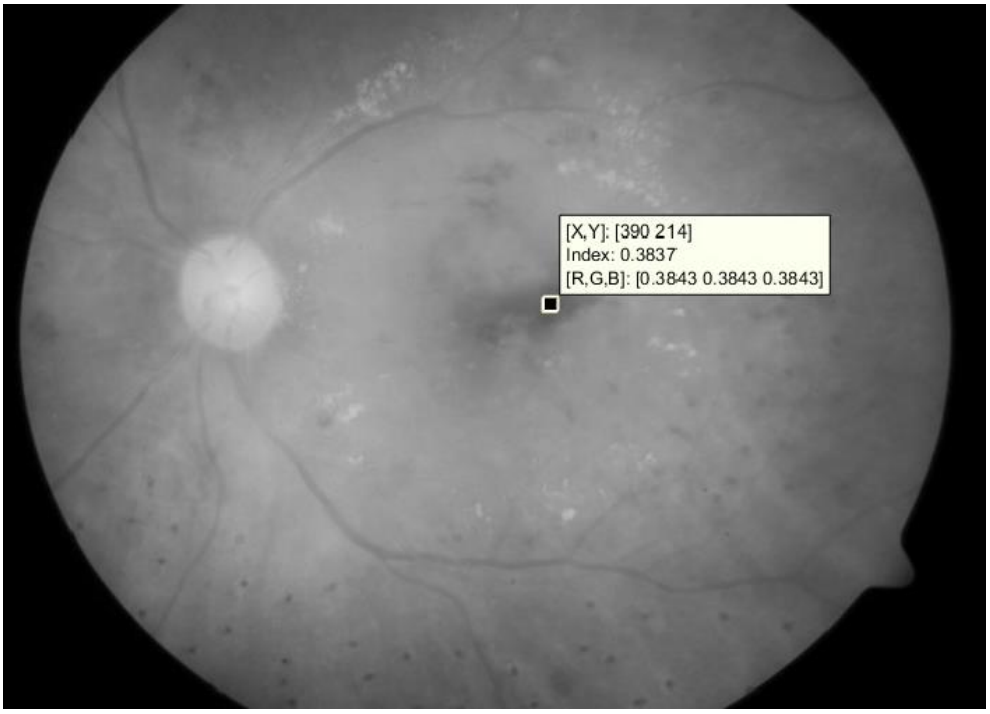


(b)

**Figure 4.6:** Pixel comparison between (a) Fovea and (b) Hemorrhage

**Exudates Analysis**

Defected = Image with exudates

Not Defected = Image without exudates

**Table 4.7:** Exudates Confusion Matrix

| | | PREDICTED | |
|---|---|---|---|
| | | Defected | Non – Defected |
| ACTUAL | Defected | 41 | 5 |
| | Non – Defected | 23 | 20 |

From the confusion matrix, the following information is extracted. Table 4.2.7 shows the corresponding table of confusion for exudates class.

**Table 4.8:** Outcome from Exudates Class

| | |
|---|---|
| True Positive (TP)<br>(actual defected image that were correctly classified as defected) | 41 |
| False Negative (FN)<br>(defected images that were incorrectly marked as non – defected images) | 5 |
| False Positive (FP)<br>(non – defected images that were incorrectly labelled as defected images) | 23 |
| True Negative (TN)<br>(all the remaining images, correctly classified as non – defected images) | 20 |

**Sensitivity, Specificity & Accuracy**

$$Sensitivity = \frac{\mathrm{TP}}{\mathrm{TP} + \mathrm{FN}}$$

$$Specificity = \frac{\mathrm{TN}}{\mathrm{FP} + \mathrm{TN}}$$

$$accuracy = \frac{\mathrm{TP}}{(\mathrm{TP} + \mathrm{FN}) + \mathrm{FP} + \mathrm{TN}}$$

To find the accuracy for the developed system, calculation is made based on the defected images.

$$Sensitivity = \frac{\mathrm{TP}}{\mathrm{TP} + \mathrm{FN}}$$
$$= \frac{41}{41 + 5}$$
$$= 0.8913$$
$$= 89.13\%$$

$$Specificity = \frac{\mathrm{TN}}{\mathrm{FT} + \mathrm{TN}}$$
$$= \frac{20}{23 + 20}$$
$$= 0.4651$$
$$= 46.51\%$$

$$Accuracy = \frac{\mathrm{TP} + \mathrm{TN}}{(\mathrm{TP} + \mathrm{FN}) + (\mathrm{FP} + \mathrm{TN})}$$
$$= \frac{41 + 20}{(41 + 5) + (23 + 20)}$$
$$= 0.6854$$

$$= 68.54\%$$

By using the developed FIA system, detection of exudates is mildly correct with the sensitivity of 89.13% and specificity of 46.51%. As for the exudates detection, this phase has low specificity due to the presence of unidentified features resembles small

black dots. This small dark disruption have sharp edges that lead to false positive detection.

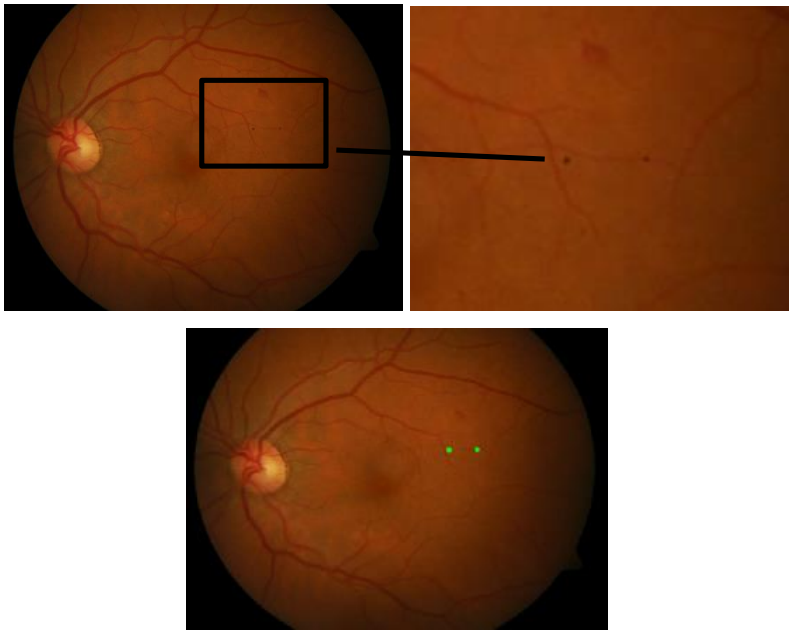

(a) Black dots and its false detection

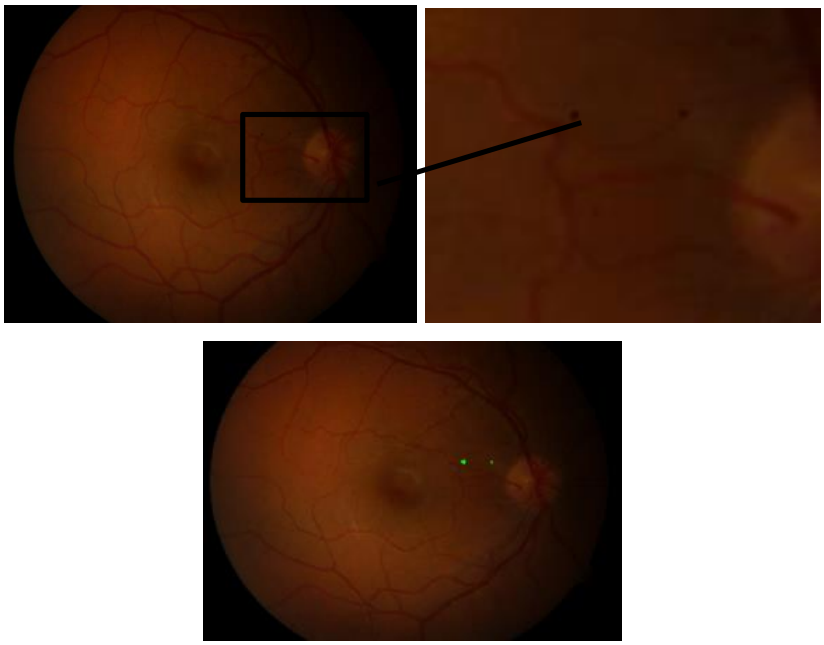

(b) Black dots and its false detection

**Figure 4.7:** False Positive detection of black dots examples images

# CHAPTER 5

# CONCLUSION AND RECCOMENDATIONS

## 5.1 CONCLUSION

In this thesis, a Fundus Image Analysis (FIA) system is developed to help an ophthalmologist gives the most accurate diagnosis of Diabetic Retinopathy. To build this system, normal and abnormal features of fundus images are extracted by developing and applying various image processing methods. This system extracts the fundal features including the retinal blood vessels, optic disk, hemorrhage and exudates through various fundus image quality such as dark images, bright images and blur images.

To assess the performance of the proposed algorithm, a dataset of 89 images is used. After being evaluated, this system however presents poor results in extracting the abnormal features as well as identifying images having diabetic retinopathy. The proposed FIA system has low accuracy for identifying fundus images with hemorrhage and exudates features with accuracy of 48.31% and 68.54% respectively. Even though the system achieved high sensitivity for detecting both abnormal features, it cannot yet be used to assist ophthalmologists in the screening and treatment of diabetic retinopathy. Sensitivity, specificity and accuracy result for both hemorrhage and exudates detection is simplified as shown in table 5.1.

**Table 5.1:** Sensitivity, Specificity and Accuracy of the System

| Features | Sensitivity (%) | Specificity (%) | Accuracy (%) |
|---|---|---|---|
| Haemorrhage | 82.69 | 0.00 | 48.31 |
| Exudates | 89.13 | 46.51 | 68.54 |

The FIA system is developed phase by phase starting with the most crucial phase which is the Masking Phase first. Masking Phase solve most of false positive detection problem. In this phase, blood vessels can be distinguish from haemorrhage and optical disk can be discriminate from exudates.

The problem that occur with the proposed algorithm is that this system cannot differentiate between haemorrhage and fovea. This anatomical feature of the eye exist in all of the fundus images and it has same colour and intensity as haemorrhage. Therefore false positive detection is very high and unpreventable. As for exudates detection case, presence of black dots disrupts the extraction process and lead to false positive results.

## 5.2 RECCOMMENDATIONS

There is still room of improvement for the developed Fundus Image Analysis system in this thesis. A few more potential algorithm can be added in order to obtain a more accurate system.

In the future, texture analysis can be applied in the system to differentiate between the anatomical feature, fovea and the abnormal feature, haemorrhage. Haemorrhage is formed from the accumulation of blood spots on the retina while fovea is a naturally existing single feature. Therefore, the spatial arrangement of colour or intensities for both features must be different. As it is known that fovea is situated at the middle of the retina, texture comparison can be done at the specified region.

# REFERENCES


Biran, A., Bidari, P. S., & Raahemifar, K. (2016). Automatic Method for Exudates and Hemorrhages Detection from Fundus Retinal Images. *World Academy of Science, Engineering and Technology, International Journal of Computer, Electrical, Automation, Control and Information Engineering, 10*(9), 1453-1456.

Bresnick, G. H., Mukamel, D. B., Dickinson, J. C., & Cole, D. R. (2000). A screening approach to the surveillance of patients with diabetes for the presence of vision-threatening retinopathy. *Ophthalmology, 107*(1), 19-24. doi:http://dx.doi.org/10.1016/S0161-6420(99)00010-X

Burhenne, L. J. W., Wood, S. A., D'Orsi, C. J., Feig, S. A., Kopans, D. B., O'Shaughnessy, K. F., . . . Castellino, R. A. (2000). Potential Contribution of Computer-aided Detection to the Sensitivity of Screening Mammography. *Radiology, 215*(2), 554-562. doi:doi:10.1148/radiology.215.2.r00ma15554

Burhenne, L. J. W., Wood, S. A., D'Orsi, C. J., Feig, S. A., Kopans, D. B., O'Shaughnessy, K. F., . . . Castellino, R. A. (2000). Potential Contribution of Computer-aided Detection to the Sensitivity of Screening Mammography. *Radiology, 215*(2), 554-562. doi:doi:10.1148/radiology.215.2.r00ma15554

Doi, K. (2007). Computer-aided diagnosis in medical imaging: Historical review, current status and future potential. *Computerized Medical Imaging and Graphics, 31*(4–5), 198-211. doi:http://dx.doi.org/10.1016/j.compmedimag.2007.02.002

Faust, O., Acharya U., R., Ng, E. Y. K., Ng, K.-H., & Suri, J. S. (2012). Algorithms for the Automated Detection of Diabetic Retinopathy Using Digital Fundus Images: A Review. *Journal of Medical Systems, 36*(1), 145-157. doi:10.1007/s10916-010-9454-7

Hipwell, J. H., Strachan, F., Olson, J. A., McHardy, K. C., Sharp, P. F., & Forrester, J. V. (2000). Automated detection of microaneurysms in digital red-free photographs: a diabetic retinopathy screening tool. *Diabetic Medicine, 17*(8), 588-594. doi:10.1046/j.1464-5491.2000.00338.x

Kamarul HG, Nurul Wahidah A, Faradila N, Rohana AK, Nor FZ, Mohd Falfazli MJ, . . . NM, L. (2016). *Computer Vision System* (1st Edition ed.). Kuantan, Pahang: Publisher Universiti Malaysia Pahang.

MathWorks. (2016a). Convert from HSV to RGB Color Space. Retrieved from https://www.mathworks.com/help/images/convert-from-hsv-to-rgb-color-space.html

MathWorks. (2016b). imregionalmin. Retrieved from https://www.mathworks.com/help/images/ref/imregionalmin.html

Mizutani, A., Muramatsu, C., Hatanaka, Y., Suemori, S., Hara, T., & Fujita, H. (2009). *Automated microaneurysm detection method based on double ring filter in retinal fundus images*.

Ravishankar, S., Jain, A., & Mittal, A. (2009, 20-25 June 2009). *Automated feature extraction for early detection of diabetic retinopathy in fundus images.* Paper presented at the 2009 IEEE Conference on Computer Vision and Pattern Recognition.

Salz, D., & Witkin, A. (2015). Imaging in diabetic retinopathy. *Middle East African Journal of Ophthalmology, 22*(2), 145-150. doi:10.4103/0974-9233.151887

Sánchez, C. I., Niemeijer, M., Dumitrescu, A. V., Suttorp-Schulten, M. S. A., Abràmoff, M. D., & van Ginneken, B. (2011). Evaluation of a Computer-Aided Diagnosis System for Diabetic Retinopathy Screening on Public Data. *Investigative Ophthalmology & Visual Science, 52*(7), 4866-4871. doi:10.1167/iovs.10-6633

Singalavanija, A., Supokavej, J., Bamroongsuk, P., Sinthanayothin, C., Phoojaruenchanachai, S., & Kongbunkiat, V. (2006). Feasibility Study on Computer-Aided Screening for Diabetic Retinopathy. *Japanese Journal of Ophthalmology, 50*(4), 361-366. doi:10.1007/s10384-005-0328-3

Sopharak, A., Uyyanonvara, B., Barman, S., & Williamson, T. H. (2008). Automatic detection of diabetic retinopathy exudates from non-dilated retinal images using mathematical morphology methods. *Computerized Medical Imaging and Graphics, 32*(8), 720-727. doi:http://dx.doi.org/10.1016/j.compmedimag.2008.08.009

Tang, L., Niemeijer, M., Reinhardt, J. M., Garvin, M. K., & Abramoff, M. D. (2013). Splat Feature Classification With Application to Retinal Hemorrhage Detection in Fundus Images. *IEEE Transactions on Medical Imaging, 32*(2), 364-375. doi:10.1109/TMI.2012.2227119

Tomi Kauppi, Valentina Kalesnykiene, Joni-Kristian Kamarainen, Lasse Lensu, Iiris Sorri, Asta Raninen, . . . Uusitalo, H. (2007). DIARETDB1 - Standard Diabetic Retinopathy Database. 2007/06/19. Retrieved from http://www.it.lut.fi/project/imageret/diaretdb1/

Vashist, P., Singh, S., Gupta, N., & Saxena, R. (2011). Role of Early Screening for Diabetic Retinopathy in Patients with Diabetes Mellitus: An Overview. *Indian J Community Med, 36*(4), 247-252. doi:10.4103/0970-0218.91324

Walter, T., Klein, J. C., Massin, P., & Erginay, A. (2002). A contribution of image processing to the diagnosis of diabetic retinopathy-detection of exudates in color fundus images of the human retina. *IEEE Transactions on Medical Imaging, 21*(10), 1236-1243. doi:10.1109/TMI.2002.806290

Wendt, G., Rönnholm, P., Heikkilä, K., & Summanen, P. (2000). A comparison between one- and two-field 60° fundus photography when screening for diabetic retinopathy. *Acta Ophthalmologica Scandinavica, 78*(1), 14-20. doi:10.1034/j.1600-0420.2000.078001014.x

Willoughby, C. E., Ponzin, D., Ferrari, S., Lobo, A., Landau, K., & Omidi, Y. (2010). Anatomy and physiology of the human eye: effects of mucopolysaccharidoses disease on structure and function – a review. *Clinical & Experimental Ophthalmology, 38*(s1), 2-11. doi:10.1111/j.1442-9071.2010.02363.x

Zhang, X., & Fan, G. (2006). Retinal Spot Lesion Detection Using Adaptive Multiscale Morphological Processing. In G. Bebis, R. Boyle, B. Parvin, D. Koracin, P. Remagnino, A. Nefian, G. Meenakshisundaram, V. Pascucci, J. Zara, J. Molineros, H. Theisel, & T. Malzbender (Eds.), *Advances in Visual Computing: Second International Symposium, ISVC 2006 Lake Tahoe, NV, USA, November 6-8, 2006. Proceedings, Part II* (pp. 490-501). Berlin, Heidelberg: Springer Berlin Heidelberg.

Zheng, L., Opas, C., & Krishnan, S. M. (1997, 30 Oct-2 Nov 1997). *Automatic image analysis of fundus photograph.* Paper presented at the Engineering in Medicine and Biology Society, 1997. Proceedings of the 19th Annual International Conference of the IEEE.

# APPENDIX A

**MATLAB Coding for Masking**

```
%% THIS IS THE OFFICIAL SCRIPT FOR PSM 2 1617/1 - SITI SARAH(ED12049)
- UNIVERSITI MALAYSIA PAHANG - FKEE
%% cleaning
%%
clc
clear all
close all

%% load image
%%
rgb = imread('image005.png');

resize = imresize(rgb,[500 700]);
figure, imshow(resize), title('select the optic disc in 4 points');

%% select optic disc - roipoly
%%
[r c] = ginput(4);
bw = roipoly(resize,r,c);

[R C] = size(bw);

for i = 1:R
    for j = 1:C
        if bw(i,j) == 1
            out(i,j) = resize(i,j);
        else
            out(i,j) = 0;
        end
    end
end


%% masking the optic disc
%%
bw2 = imcomplement(out);
imwrite(bw2, 'optic disc mask.png')
figure, suptitle('masking the optic disc')
subplot(221), imshow(bw), title('selected region')
subplot(222), imshow(bw2), title('complemented region')

im_gray = rgb2gray(resize);
subplot(223), imshow(im_gray), title('grayscale image')
```

```
retina = uint8(im_gray);
optic_disc = uint8(bw2);
mask_optic_disc = immultiply(retina,optic_disc);
subplot(224), imshow(mask_optic_disc), title('masked optic disc image')

imwrite(mask_optic_disc,'masked optic disc.png')

%% masking retina background
%%
mask = (resize(:,:,1) == 0) & (resize(:,:,2) == 0) & (resize(:,:,3) == 0);

se = strel('disk', 20);
mask_dilate = imdilate(mask,se);
figure, suptitle('masking the retinal background')
subplot(131), imshow(rgb), title('original image')
subplot(132), imshow(mask), title('all channel = 0')

mask_bw = im2bw(mask_dilate);
mask_bw2 = imcomplement(mask_bw);
subplot(133), imshow(mask_bw2), title('complemented - background mask')

mask2 = imcrop(mask_bw2, [1 10 700 700]);
mask3 = imcrop(mask2, [1 0 700 510]);

mask_bw3 = im2bw(mask3);
mask_background = imresize(mask_bw3, [500 700]);

imwrite(mask_background, 'fmask.png')

%% masking the blood vessel
%%
g = resize(:,:,2);
g2 = imcomplement(g);
figure, suptitle('masking the blood vessel')
subplot(251), imshow(g), title('green channel')
subplot(252), imshow(g2), title('complemented green channel')

ahe = adapthisteq(g2);
subplot(253), imshow(ahe), title('clahe')

se2 = strel('ball',8,8);
g2open = imopen(ahe,se2);
g2odisk = ahe - g2open;
subplot(254), imshow(g2open), title('opening')
subplot(255), imshow(g2odisk), title('optic disc removed')

medfilt = medfilt2(g2odisk);
```

```
background = imopen(medfilt, se);
medfilt_2 = medfilt - background;
im_adjust = imadjust(medfilt_2);
subplot(256), imshow(medfilt), title('median filtering')
subplot(257), imshow(background), title('opening')
subplot(258), imshow(medfilt_2), title('background removed')

level = graythresh(im_adjust);
bw3 = im2bw(im_adjust,level);
bw3 = bwareaopen(bw3, 30);
subplot(259), imshow(bw3), title('thresholding')

se3 = strel('disk',3);
bw3_dilate = imdilate(bw3,se3);
bw3_dilate = imcomplement(bw3_dilate);
subplot(2,5,10), imshow(bw3_dilate), title('dilated')

imwrite(bw3_dilate, 'blood vessel mask.png')

%% complete masking
%%
optic_disc2 = imread('optic disc mask.png');
blood_vessel = imread('blood vessel mask.png');
a = uint8(optic_disc2);
b = uint8(blood_vessel);
mask4 = immultiply(a, b);
figure, suptitle('full mask - image multiply')
subplot(131), imshow(mask4), title('optic disc + blood vessel')

imwrite(mask4, 'masked retina.png')

bin_mask = im2bw(mask4);
mask_background2 = imread('fmask.png');
c = uint8(mask4);
d = uint8(mask_background2);
full_mask = immultiply(c, d);
subplot(132), imshow(full_mask), title('with background mask')
imwrite(full_mask,'fullmask.png')
bin_mask2 = im2bw(full_mask);
subplot(133), imshow(bin_mask2), title('binary mask')

imwrite(bin_mask2,'binary mask.png')

%% END %%
```

# APPENDIX B

**MATLAB Coding for Hemorrhage Detection**

```
%% THIS IS THE OFFICIAL SCRIPT FOR PSM 2 1617/1 - SITI SARAH(ED12049)
- UNIVERSITI MALAYSIA PAHANG - FKEE
%% 1. cleaning
%%
clc
clear all
close all

%% 2. load image
%%
rgb = imread('image005.png');
resize = imresize(rgb,[500 700]);

%% 3. hsv
%%
hsv = rgb2hsv(resize);
hsv(:,:,1)= .2;
hsv(:,:,2)= 1;
resize2 = hsv2rgb(hsv);
figure, imshow(resize2), title('saturation adjust')
%% grayscale
%%
imgray = rgb2gray(resize2);
figure, imshow(imgray), title('grayscale')

%% morphological opening - erode
%%
se = strel('disk',19);
Io = imopen(imgray, se);
figure, imshow(Io), title('opening')

Ie = imerode(imgray, se);
Iobr = imreconstruct(Ie, imgray);
figure, imshow(Iobr), title('erode')


%% morphological closing - dilate
%%
Ioc = imclose(Io, se);

figure, imshow(Ioc), title('closing')

se2 = strel('disk', 5);
Iobrd = imdilate(Iobr, se2);
```

```
figure, imshow(Iobr), title('dilate')

Iobrcbr = imreconstruct(imcomplement(Iobrd), imcomplement(Iobr));
Iobrcbr = imcomplement(Iobrcbr);

figure, imshow(Iobrcbr), title('oecd')
%% extracting the hemorrhage
%%
fgm = imregionalmin(Iobrcbr);


figure, imshow(fgm), title('Regional minima')

%% marking the hemorrhage
%%
bw2 = im2bw (fgm, 1);
% subplot(349),imshow (bw2), title('extracted hemorrhages'), impixelinfo;

mask = imread('binary mask.png');
b = uint8(mask);
c = uint8(bw2);
masked = immultiply(b,c);
figure, imshow(masked), title('masked')

IB=~masked;
figure, imshow (IB), title('complemented'), impixelinfo;

[B,L] = bwboundaries(IB,'holes');
figure, imshow(label2rgb(L, @gray, [.5 .5 .5])), title('labeled'), impixelinfo;
figure, imshow(resize), title('marked are detected exudates')


hold on

for k = 1:length(B)
   boundary = B{km;
   plot(boundary(:,2), boundary(:,1), 'b', 'LineWidth', 1.5)
end

%% information
%%
cc = bwconncomp(masked)
labeled = labelmatrix(cc);

stats = regionprops(L,'Area', 'Perimeter', 'PixelList')

%% END %%
```

# APPENDIX C

**MATLAB Coding for Exudates Detection**

```
%% THIS IS THE OFFICIAL SCRIPT FOR PSM 2 1617/1 - SITI SARAH(ED12049)
- UNIVERSITI MALAYSIA PAHANG - FKEE
%% cleaning
%%
clc
clear all
close all

%% load image
%%
rgb = imread('image005.png');
resize = imresize(rgb,[500 700]);

g = resize(:,:,2);
figure, suptitle('Exudates Extraction')
subplot(241), imshow(g), title('green channel')
%% filtering
%%
hy = fspecial('prewitt');
hx = hy';
Iy = imfilter(double(g), hy, 'replicate');
Ix = imfilter(double(g), hx, 'replicate');
subplot(242), imshow(Iy), title('prewitt filter 1')
subplot(243), imshow(Ix), title('prewitt filter 2')

%% gradient magnitude
%%
gradmag = sqrt(Ix.^2 + Iy.^2);
subplot(244), imshow(gradmag,[]), title('Gradient magnitude')

%% masking
%%
mask = imread('binary mask.png');
a = uint8(mask);
b = uint8(gradmag);
masked = immultiply(a,b);
subplot(245), imshow(masked), title('masked gradmag')

%% exudates extraction - region of interest
%%
bw = roicolor(masked,70,155);
subplot(246), imshow(bw), title('extracted exudates')

%% mark the extracted exudates
```

```
%%

[B,L] = bwboundaries(bw,'holes');
subplot(247),imshow(label2rgb(L, @gray, [.5 .5 .5])), title('labeled'), impixelinfo;
subplot(248),imshow(resize), title('marked are detected exudates')
hold on

for k = 1:numel(B)
   plot(B{k}(:,2), B{k}(:,1), 'g', 'Linewidth', 1)
end

%% information
%%
cc = bwconncomp(L)
labeled = labelmatrix(cc);

stats = regionprops(L,'Area', 'Perimeter')
%% END %%
```

# APPENDIX D

**MATLAB Coding for GUI**

```
  %% THIS IS THE OFFICIAL SCRIPT FOR PSM 2 1617/1 - SITI SARAH(ED12049)
- UNIVERSITI MALAYSIA PAHANG - FKEE
%%
function varargout = GUI(varargin)
% GUI MATLAB code for GUI.fig
%      GUI, by itself, creates a new GUI or raises the existing
%      singleton*.
%
%      H = GUI returns the handle to a new GUI or the handle to
%      the existing singleton*.
%
%      GUI('CALLBACK',hObject,eventData,handles,...) calls the local
%      function named CALLBACK in GUI.M with the given input arguments.
%
%      GUI('Property','Value',...) creates a new GUI or raises the
%      existing singleton*.  Starting from the left, property value pairs are
%      applied to the GUI before GUI_OpeningFcn gets called.  An
%      unrecognized property name or invalid value makes property application
%      stop.  All inputs are passed to GUI_OpeningFcn via varargin.
%
%      *See GUI Options on GUIDE's Tools menu.  Choose "GUI allows only one
%      instance to run (singleton)".
%
% See also: GUIDE, GUIDATA, GUIHANDLES

% Edit the above text to modify the response to help GUI

% Last Modified by GUIDE v2.5 27-Nov-2016 22:35:39

% Begin initialization code - DO NOT EDIT
gui_Singleton = 1;
gui_State = struct('gui_Name',       mfilename, ...
                   'gui_Singleton',  gui_Singleton, ...
                   'gui_OpeningFcn', @GUI_OpeningFcn, ...
                   'gui_OutputFcn',  @GUI_OutputFcn, ...
                   'gui_LayoutFcn',  [] , ...
                   'gui_Callback',   []);
if nargin && ischar(varargin{1})
    gui_State.gui_Callback = str2func(varargin{1});
end

if nargout
    [varargout{1:nargout}] = gui_mainfcn(gui_State, varargin{:});
else
```

```
    gui_mainfcn(gui_State, varargin{:});
end
% End initialization code - DO NOT EDIT


% --- Executes just before GUI is made visible.
function GUI_OpeningFcn(hObject, eventdata, handles, varargin)
% This function has no output args, see OutputFcn.
% hObject    handle to figure
% eventdata  reserved - to be defined in a future version of MATLAB
% handles    structure with handles and user data (see GUIDATA)
% varargin   command line arguments to GUI (see VARARGIN)

% Choose default command line output for GUI
handles.output = hObject;

% Update handles structure
guidata(hObject, handles);

% UIWAIT makes GUI wait for user response (see UIRESUME)
% uiwait(handles.figure1);


% --- Outputs from this function are returned to the command line.
function varargout = GUI_OutputFcn(hObject, eventdata, handles)
% varargout  cell array for returning output args (see VARARGOUT);
% hObject    handle to figure
% eventdata  reserved - to be defined in a future version of MATLAB
% handles    structure with handles and user data (see GUIDATA)

% Get default command line output from handles structure
varargout{1} = handles.output;


% --- Executes on button press in pushbutton1.
function pushbutton1_Callback(hObject, eventdata, handles)
% hObject    handle to pushbutton1 (see GCBO)
% eventdata  reserved - to be defined in a future version of MATLAB
% handles    structure with handles and user data (see GUIDATA)
global rgb

[path, user_cancel] = imgetfile();
if user_cancel
    msgbox(sprintf('Error'), 'Error','Error');
return
end
rgb = imread(path);
im = imresize(rgb,[500 700]);
axes(handles.axes1), imshow(im);
```

```
%%
%--- Executes on button press in pushbutton2.
function pushbutton2_Callback(hObject, eventdata, handles)
% hObject    handle to pushbutton2 (see GCBO)
% eventdata  reserved - to be defined in a future version of MATLAB
% handles    structure with handles and user data (see GUIDATA)
global rgb
%% roipoly -- select optic disc manually
%%
im = imresize(rgb,[500 700]);
axes(handles.axes6),imshow(im);

[r c] = ginput(4);
bw = roipoly(im,r,c);
% figure, imshow(bw) %show selected shape

[R C] = size(bw);

for i = 1:R
   for j = 1:C
      if bw(i,j) == 1
         out(i,j) = im(i,j);
      else
         out(i,j) = 0;
      end
   end
end

% figure, imshow(out,[]) %show selected region image

%save the selected region
% imwrite(out,'selected region.png')
%% masking the retina
%%
mask = (im(:,:,1) == 0) & (im(:,:,2) == 0) & (im(:,:,3) == 0);
% figure, imshow(mask)

se = strel('disk', 65);
maskIdx = imdilate(mask,se);
% figure, imshow(maskIdx)

mask_bw = im2bw(maskIdx);
mask_bw2 = imcomplement(mask_bw);
% figure, imshow(mask_bw2)

mask2 = imcrop(mask_bw2, [1 20 700 700]);
% figure, imshow(mask2)

mask3 = imcrop(mask2, [1 0 700 470]);
```

```
mask3_2 = im2bw(mask3);
mask3_3 = imresize(mask3_2, [500 700]);
% figure, imshow(mask3_3)
imwrite(mask3_3, 'fmask.png')
%% masking the optic disc
%%
bw2 = imcomplement(out);
imwrite(bw2, 'optic disc mask.png')

im2 = rgb2gray(im);

im_gray = uint8(im2);
mask4 = uint8(bw2);

im3 = immultiply(im_gray,mask4);
% figure, imshow(im3), title('masked optic disc')
imwrite(im3,'masked optic disc.png')
%% blood vessel masking
%%
g = im(:,:,2); %select green channel
g2 = imcomplement(g);

% figure,
% subplot(121), imshow(g), title('green channel')
% subplot(122), imshow(g2), title('inversed green channel')

ahe = adapthisteq(g2);
% figure, imshow(g2)
se2 = strel('ball',8,8);
gopen = imopen(ahe,se2);
godisk = ahe - gopen;

% figure,
% subplot(131), imshow(ahe), title('adaptive histogram equalization')
% subplot(132), imshow(gopen), title('gopen')
% subplot(133), imshow(godisk), title('godisk')

medfilt = medfilt2(godisk);
background = imopen(medfilt,strel('disk',20));
im4 = medfilt - background;
im5 = imadjust(im4);

% figure,
% subplot(131), imshow(medfilt), title('2D median filter')
% subplot(132), imshow(im4), title('background removed')
% subplot(133), imshow(im5), title('background removed - adjusted')

level = graythresh(im5);
bw3 = im2bw(im5,level);
bw3 = bwareaopen(bw3, 30);
```

```
se3 = strel('disk',3);
bw4 = imdilate(bw3,se3);

bw4 = imcomplement(bw4);
imwrite(bw4, 'blood vessel mask.png')

% figure,
% subplot(121), imshow(bw3), title('detected blood vessel')
% subplot(122), imshow(bw4), title('blood vessel mask')
%% form a complete mask (optic disc + blood vessel + retina)
%%
OD = imread('optic disc mask.png');
BV = imread('blood vessel mask.png');
I = uint8(OD);
J = uint8(BV);
im6 = immultiply(I, J);
imwrite(im6, 'masked retina.png')

% figure, imshow(im6), title('masked retina')

bin_mask = im2bw(im6);
% figure, imshow(bin_mask)
axes(handles.axes2), imshow(im6);

im7 = imread('fmask.png');
L = uint8(im6);
M = uint8(im7);
im8 = immultiply(L, M);
% figure, imshow(im8)
imwrite(im8, 'fullmask.png'),

bin_mask2 = im2bw(im8);
imwrite(bin_mask2,'binary mask.png')

%%
% --- Executes on button press in pushbutton3.

function pushbutton3_Callback(hObject, eventdata, handles)
% hObject    handle to pushbutton3 (see GCBO)
% eventdata  reserved - to be defined in a future version of MATLAB
% handles    structure with handles and user data (see GUIDATA)

%% 1. load image
%%
global rgb

%% 2. load image
%%
resize = imresize(rgb,[500 700]);
```

```
%% 3. hsv
%%
hsv = rgb2hsv(resize);
hsv(:,:,1)= .2;
hsv(:,:,2)= 1;
resize2 = hsv2rgb(hsv);
% figure,
% subplot(341), imshow(resize2), title('saturation adjust')
%% grayscale
%%
imgray = rgb2gray(resize2);
% subplot(342), imshow(imgray)

%% morphological opening - erode
%%
se = strel('disk',19);
Io = imopen(imgray, se);
% subplot(343), imshow(Io), title('opening')

Ie = imerode(imgray, se);
Iobr = imreconstruct(Ie, imgray);
% subplot(344), imshow(Iobr), title('erode')


%% morphological closing - dilate
%%
Ioc = imclose(Io, se);

% subplot(345), imshow(Ioc), title('closing')

se2 = strel('disk',5);
Iobrd = imdilate(Iobr, se2);
% subplot(346), imshow(Iobr), title('dilate')

Iobrcbr = imreconstruct(imcomplement(Iobrd), imcomplement(Iobr));
Iobrcbr = imcomplement(Iobrcbr);

% subplot(347), imshow(Iobrcbr), title('oecd')
%% extracting the hemorrhage
%%
fgm = imregionalmin(Iobrcbr);

% subplot(348),imshow(fgm), title('Regional minima')

%% marking the hemorrhage
%%
bw2 = im2bw (fgm, 1);
% subplot(349),imshow (bw2), title('extracted hemorrhages'), impixelinfo;
```

```
mask = imread('binary mask.png');
b = uint8(mask);
c = uint8(bw2);
masked = immultiply(b,c);
% subplot(349), imshow(masked), title('masked')

IB=~masked;
% subplot(3,4,10),imshow (IB), title('complemented'), impixelinfo;

[B,L] = bwboundaries(IB,'holes');
% subplot(3,4,11),imshow(label2rgb(L, @gray, [.5 .5 .5])), title('labeled'), impixelinfo;
axes(handles.axes3),imshow(resize);

hold on

for k = 1:length(B)
   boundary = B{k};
   plot(boundary(:,2), boundary(:,1), 'b', 'LineWidth', 1.5)
end

%% information
%%
cc = bwconncomp(masked)
labeled = labelmatrix(cc);

stats = regionprops(L,'Area', 'Perimeter')

%% END %%


%% information
%%
cc = bwconncomp(masked)
labeled = labelmatrix(cc);

stats = regionprops(L,'Area', 'Perimeter')

%% END %%



%%
% --- Executes on button press in pushbutton4.
function pushbutton4_Callback(hObject, eventdata, handles)
% hObject    handle to pushbutton4 (see GCBO)
% eventdata  reserved - to be defined in a future version of MATLAB
% handles    structure with handles and user data (see GUIDATA)
global rgb

%% load image
```

```
%%
resize = imresize(rgb,[500 700]);

g = resize(:,:,2);

%% filtering
%%
hy = fspecial('prewitt');
hx = hy';
Iy = imfilter(double(g), hy, 'replicate');
Ix = imfilter(double(g), hx, 'replicate');

%% gradient magnitude
%%
gradmag = sqrt(Ix.^2 + Iy.^2);

%% masking
%%
mask = imread('binary mask.png');
a = uint8(mask);
b = uint8(gradmag);
masked = immultiply(a,b);

%% exudates extraction - region of interest
%%
bw = roicolor(masked,70,155);

%% mark the extracted exudates
%%
c = bwboundaries(bw);
axes(handles.axes4),imshow(resize);
% figure,imshow(resize), title('extracted exudates')
hold on

for k = 1:numel(c)
   plot(c{k}(:,2), c{k}(:,1), 'g', 'Linewidth', 1.5)
end

%% END %%

%%
% --- Executes on button press in pushbutton6.
function pushbutton6_Callback(hObject, eventdata, handles)
% hObject    handle to pushbutton6 (see GCBO)
% eventdata  reserved - to be defined in a future version of MATLAB
% handles    structure with handles and user data (see GUIDATA)
cla(handles.axes1, 'reset')
cla(handles.axes2, 'reset')
cla(handles.axes3, 'reset')
cla(handles.axes4, 'reset')
```

```
cla(handles.axes6, 'reset')


% --- Executes when figure1 is resized.
function figure1_SizeChangedFcn(hObject, eventdata, handles)
% hObject    handle to figure1 (see GCBO)
% eventdata  reserved - to be defined in a future version of MATLAB
% handles    structure with handles and user data (see GUIDATA)
```